Progress In Electromagnetics Research B, Vol. 64, 145–170, 2015

A New Class of Adaptive CFAR Methods for Nonhomogeneous Environments

Anatolii A. Kononov*, Jin-Ha Kim, Jin-Ki Kim, and Gyoungju Kim

Abstract—The paper introduces a new class of adaptive CFAR methods to cope with the problem of outliers due to the presence of clutter edges and interfering targets. A fundamental distinction between the proposed approach and existing adaptive CFAR approaches is that in order to maintain robust performance the former uses information on positions at which estimated outlier-free cells appear in the full reference window and the statistics of the sample in the cell under test. The performance of one of the possible implementations of new adaptive CFAR methods is studied and compared with that of an existing adaptive CFAR approach. The results show significant advantages of the proposed class of adaptive CFAR methods in both the false alarm regulation property and detection performance.

1. INTRODUCTION

Constant false alarm rate (CFAR) methods are widely adopted in radar target detection when all the parameters in the statistical distributions characterizing background are not known and may be nonstationary. To maintain the false alarm rate at specified constant level CFAR methods set the detection threshold on a cell-by-cell basis using estimates of total interference (noise-plus-clutter) power in the vicinity of the cell under test (CUT). These estimates are derived by processing a set of samples of the background in the range interval surrounding the CUT. Such a group of samples is herein referred to as reference samples or full reference window. Under the assumption that the background is homogeneous, i.e., represented by samples that are statistically independent and identically distributed random variables, the basic method, known as cell averaging (CA) CFAR, is to set a detection threshold based on averaging the samples from a predetermined full reference window centered on the CUT. As is well known when the background is not homogeneous the detection and false alarm performance of the CA-CFAR method are seriously degraded [1, 2].

Two major operational environments, when the assumption of homogeneous reference window is violated, are those presented by regions of clutter power transition (clutter edges) and by interfering targets (multiple target environments). The presence of interfering targets or clutter edges is known to be a particular problem in CFAR processing because of lack of homogeneity in the reference window [1, 2]. The samples that appear in the reference window due to the presence of clutter or interfering targets and destroy the homogeneity are hereinafter referred to as outliers.

Various modifications have been applied to the CA-CFAR method to improve the detection and false alarm performance in nonhomogeneous environments. One class of such modifications is known as robust CFAR methods that are devised to achieve acceptable CFAR performances under specific heterogeneous conditions [1, 2]. This class includes widely known CFAR methods such as greatest-of CA-CFAR, smallest-of CA-CFAR, trimmed mean (TM) or censored (CS) CFAR, and order statistics (OS) CFAR. The robust CFAR methods have a significant shortcoming: they rely heavily on a priori

Received 16 September 2015, Accepted 13 November 2015, Scheduled 9 December 2015

* Corresponding author: Anatolii A. Kononov (akononov@onestx.com).

The authors are with Research Center, STX Engine, 288, Guseong-ro, Giheung-gu, Yongin-si, Gyeonggi-do, 446–915, Republic of Korea.

knowledge of the interference environment, which is required for determining the most suitable CFAR method and its parameters.

More attractive class of CFAR techniques that are devised to overcome the problem of a prior uncertainty includes adaptive CFAR methods [1], which adaptively adjust CFAR parameters based on the measured data rather than on the assumptions concerning the environment. Over the past three decades, quite a number of adaptive CFAR methods have been reported in the literature. Analysis of the published adaptive methods shows that the majority of them completely ignore information on the positions of reference samples representing homogeneous background around the CUT while others use rough form of this information. Thus the approaches proposed in [3–6] are based on estimating the position of only one of the reference samples which indicates the location of a possible clutter edge or a group of the samples due to interfering targets.

This paper introduces an approach that gives rise to a new class of adaptive CFAR methods. A distinctive feature of this approach is that it is essentially based on using all available information on the positions at which the estimated outlier-free samples appear in the full reference window and the statistics of the sample in the test cell. We analyze the performance of one of the possible implementations of the proposed approach and demonstrate its advantages against an adaptive CFAR detector suggested in [3]. That adaptive detector is only one of the known adaptive CFAR schemes employing coarse information on location of the outlier-free reference samples, which addresses both the clutter edge and interfering targets problem.

Generally speaking, three modifications of adaptive CFAR methods have been proposed in [3]. First one, which is referred to as GO/SO CFAR detector (it selects either a group of the smallest samples or a group of the largest samples in the full reference window), is designed to address the clutter edge problem. Second one, which is referred to as ACMLD (automatic censored mean level detector), is designed to address the problem of interfering targets. Third modification that is referred to as GTL-CMLD (generalized two-level censored mean level detector) addresses both clutter edge and interfering targets problem.

The methods proposed in [3] operate on the measured data with no assumption concerning the number of outliers in the full reference window. To estimate the number of outliers and to determine whether the CUT is in the outlier or in the clear (noise) region all these methods employ an automatic censoring procedure that operates on the ordered sequence of the reference samples, which are ranked in ascending order according to their magnitudes.

With the GO/SO CFAR detector the following decision rule is used to determine whether the CUT is in the clutter or in the clear, provided that the total number of reference samples M is even: if the estimated number of outliers $\hat{r} < M/2$ the CUT is decided to be in the clear, otherwise the CUT is decided to be in the clutter. If the CUT is declared to be in the clear, the samples that supposedly represent the clutter region are censored. Otherwise, if the CUT is declared to be in the clutter, the samples that supposedly represent the clear region are censored. The uncensored samples, which supposedly represent the homogeneous noise background around the CUT, are then combined to estimate the average background power that is used to generate the adaptive detection threshold. It should be noted that the decision rule used in GO/SO CFAR detector and that in other adaptive CFAR detectors proposed in [3] assumes that only one clutter edge is present in the full reference window.

The ACMLD uses the same censoring procedure to estimate the number of outliers; however, in this case the higher ordered samples are always censored since the CUT sample is assumed in [3] to be identically distributed with the noise in all other reference samples.

To cope with both of the clutter edge and interfering targets problem the GTL-CMLD detector combines the decision rules of the GO/SO CFAR and the ACMLD detector. So, in case of the GTL-CMLD the censoring procedure may run two times. If on the first run the estimated number of outliers $\hat{r} < M/2$, the decision rule of the GO/SO CFAR detector is applied, i.e., the CUT decided to be in the clear, then $M - \hat{r}$ samples (that supposedly are from the clear) are used in computing the detection threshold and the censoring procedure stops, otherwise, i.e., if $\hat{r} \geq M/2$, the censoring procedure runs again using the $\hat{r}$ ordered samples (that supposedly represent all outliers) as a new censoring window and the decision rule of the ACMLD is applied. That is, if the censoring procedure determines that these $\hat{r}$ samples contain $\hat{q}$ outliers, i.e., samples that are drawn from a distribution with higher average power, then all these $\hat{q}$ outliers are censored and only $\hat{r} - \hat{q}$ samples from a distribution with lower

average power are used in computing the detection threshold since the CUT is assumed to be always from the distribution with lower average power. If the censoring procedure determines that all the $\hat{r}$ samples are drawn from one distribution then no samples are censored and all these $\hat{r}$ samples are used in computing the detection threshold.

Although the GTL-CMLD detector, as well as the GO/SO CFAR and ACMLD detector, operates with no a priori information on the number of outliers these techniques are not free of disadvantages. In this Section we discuss these CFAR detectors upon ideal condition that the number of outliers is estimated with no errors. Further in Subsection 2.3 we prove that the errors in estimating the number of outliers may result in serious degradation of the false alarm regulation property of the GTL-CMLD detector.

The ACMLD is impractical in scenarios when clutter edge is present in the reference window. Since this detector always selects the samples from a distribution with lower average power its false alarm performance in clutter may seriously be degraded if the number of outliers due to clutter in the reference window exceeds $M/2$ (one of the possible scenarios is shown in Figure 1). In this scenario the CUT is in clutter but with high probability the detection threshold is computed using the samples from the clear. Hence, the detection threshold is unacceptably lowered and the false alarm probability is significantly increased.

The detection and false alarm performance of the GO/SO CFAR detector may also degrade seriously. For instance, in multiple target environments its detection performance degrades unacceptably when the number of outliers exceeds $M/2$ and the CUT is in the clear as is shown in Figure 2(a). This scenario is typical for marine radars operating in fishing areas overcrowded with small ships and boats. From Figure 2(b), it is seen that the GO/SO CFAR detector declares with high probability that the

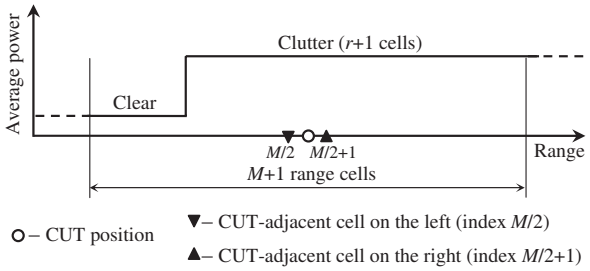

Figure 1. Clutter power transition with one edge.

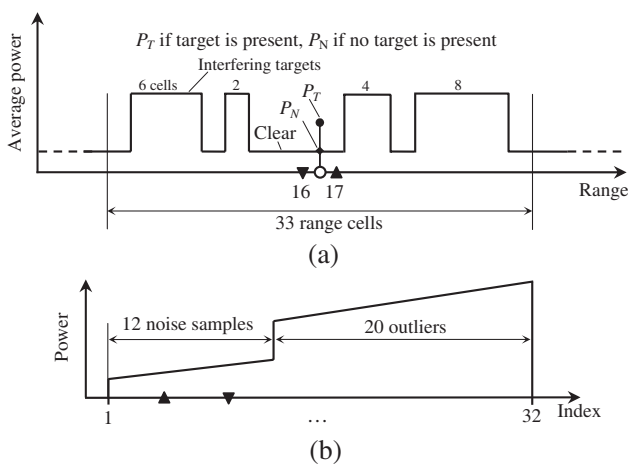

Figure 2. Dense multiple target environment. (a) Interfering targets in the full reference window. (b) Reference samples after sorting.

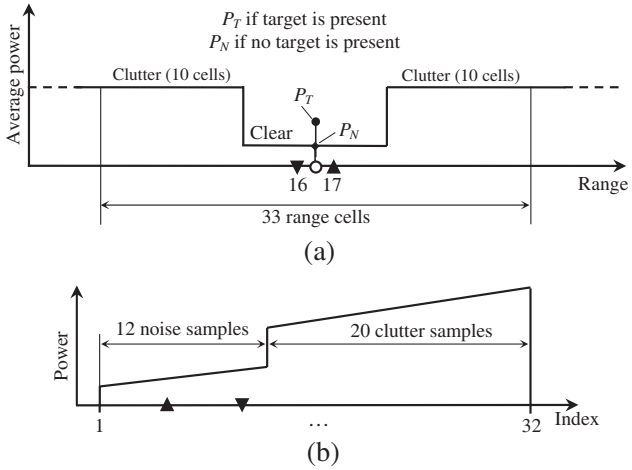

Figure 3. Clutter power transition with two edges. (a) Two clutter edges, CUT and two adjacent cells are in clear. (b) Reference samples after sorting.

CUT is in the outlier region. Hence, the outliers are used to estimate the average background power. The average power of outliers may be significantly higher than that of the CUT. Thus, the threshold is raised unnecessarily and therefore the probability of detection as well as the false alarm probability is significantly lowered.

It is also clear from the previous discussion that the detection and false alarm performance of the GO/SO CFAR detector are seriously degraded when two clutter edges are present in the reference window, the number of outliers exceeds $M/2$ and the CUT resides in the clear. This kind of scenario is shown in Figure 3(a). Moreover, the false alarm probability of the GO/SO CFAR detector is intolerably increased in case of two clutter edges even when the number of clutter samples in the reference window is less than $M/2$ and the CUT is in the clutter as shown in Figure 4(a).

In this scenario, the censoring algorithm with high probability decides that the CUT is in clear although the CUT is actually in the clutter. This is obvious from Figure 4(b) representing the ordered reference samples that used as an input to the censoring algorithm. Hence, the noise samples are used to estimate the average background power. The average power of noise samples may be significantly lower than the actual clutter power in the CUT. Thus, the threshold is significantly lowered and the false alarm probability is increased intolerably.

The GTL-CMLD detector is free of the disadvantages of the ACMLD and GO/SO CFAR detector in scenarios similar to that shown in Figure 1 (on the assumption that the number of outliers is estimated with no error) but it has the other disadvantages of the GO/SO CFAR detector in scenarios similar to those shown in Figure 2(a), Figure 3(a) and Figure 4(a). For example, consider scenario depicted in Figure 5(a), where the interfering targets are present in the full reference window in addition to the clutter. From Figure 5(b), it is seen that according to the decision strategy adopted for the GTL-CMLD, the CUT is decided to be in the clutter even if it actually is in the clear. Thus, the threshold is raised unnecessarily and the detection probability, as well as the probability of false alarm, is significantly lowered.

The main idea of this paper originates from the intention to get rid of disadvantages of the GTL-CMLD detector by incorporating in CFAR detection process such additional information that allow ensuring robust false alarm and detection performance in the presence of two or more clutter edges and/or in multiple target environments. Obviously, for achieving robust false alarm performance it

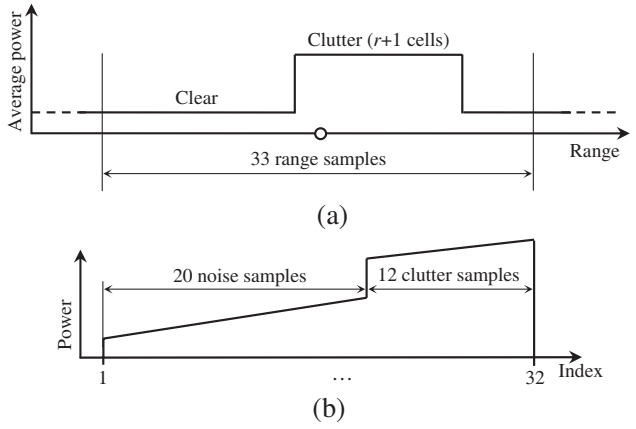

Figure 4. Clutter patch of a limited extent. (a) CUT and two adjacent cells are in clutter. (b) Reference samples after sorting, $r = 12$.

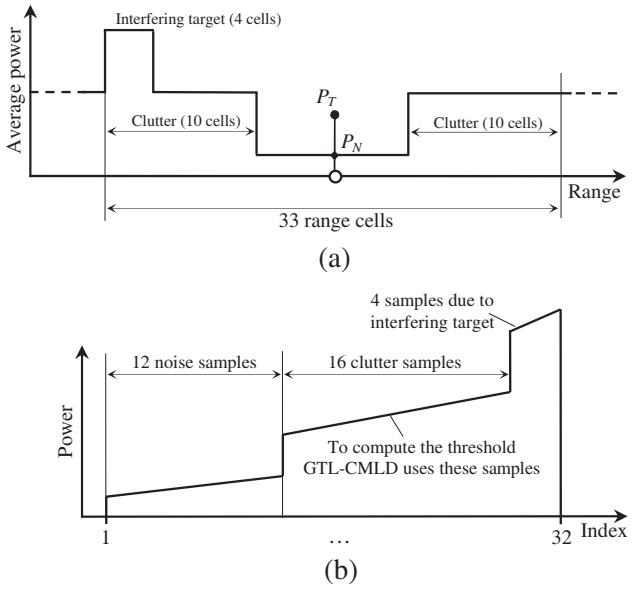

Figure 5. Clutter power transition with two edges and interfering targets. (a) Clutter and interfering targets, CUT in clear. (b) Reference samples after sorting.

is necessary to find within the full reference window a subset of homogeneous (outlier-free) reference samples having a distribution which is equal to that of the CUT and to use that subset for computing the adaptive threshold. This subset of reference samples is referred to as *adaptive reference window*.

To determine the proper adaptive reference window our approach suggests using the magnitude of the sample in the test cell and all the subsets of outlier-free samples along with corresponding subsets that represent the positions (indices) at which the samples of each subset appear in the full reference window. For this reason, CFAR methods based on the proposed approach are referred to as adaptive *Outlier-Free Positions Identification CFAR* (OFPI-CFAR) algorithms.

In Section 2, we introduce a concept of outlier-free (homogeneous) regions when the outliers due to clutter and interfering targets are present in the full reference window and consider one possible implementation of the proposed adaptive OFPI-CFAR. In Section 3, the performance of this implementation is evaluated and compared with that of the GTL-CMLD detector. To evaluate the performance we carry out statistical simulations using an approach suggested in Appendix D. Finally, we conclude our discussions in Section 4.

2. ADAPTIVE OFPI-CFAR PROCESSING

2.1. Possible Implementation

The main concept of the adaptive OFPI-CFAR is to employ the statistics of the CUT sample and all available information on the positions of the homogeneous (outlier-free) samples around the CUT in order to properly identify an adaptive reference window which is free of outliers due to clutter edges and/or interfering targets. It is clear that using outlier-free adaptive reference window allows eliminating the detrimental effect of outliers on the adaptive CFAR threshold and, finally, on the detection and false alarm performance. To characterize the homogeneity of the full reference window we use the notions of the noise (clear), clutter, and interferer regions for the reference samples, which we denote by S_n, S_c, and S_i, respectively. Figure 6 illustrates these regions using a sequence of sorted reference samples with no samples intermixing between different regions for the general case when the outliers due to clutter edge and interfering targets are present in the full reference window; r denotes the true total number of outliers (clutter plus interfering targets) and q is the true number of outliers due to interfering targets (average clutter power is assumed to be lower than that of interfering targets). In particular cases, e.g., when only clutter outliers are present the homogeneity of the full reference window is characterized by the clear and clutter regions S_n and S_c. Obviously, that if no clutter samples and interfering targets are present in the full reference window its homogeneity region is represented by all the reference samples.

Figure 7 shows a possible implementation of the adaptive OFPI-CFAR. The input samples x_i,

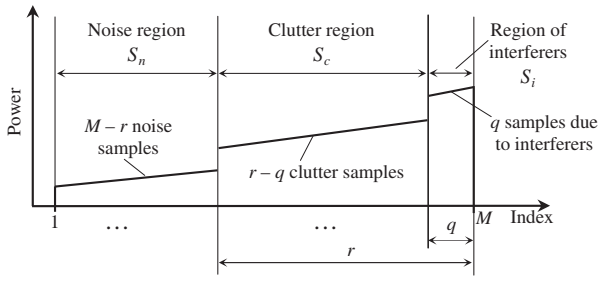

Figure 6. Regions of homogeneity represented by noise, clutter and interfering targets.

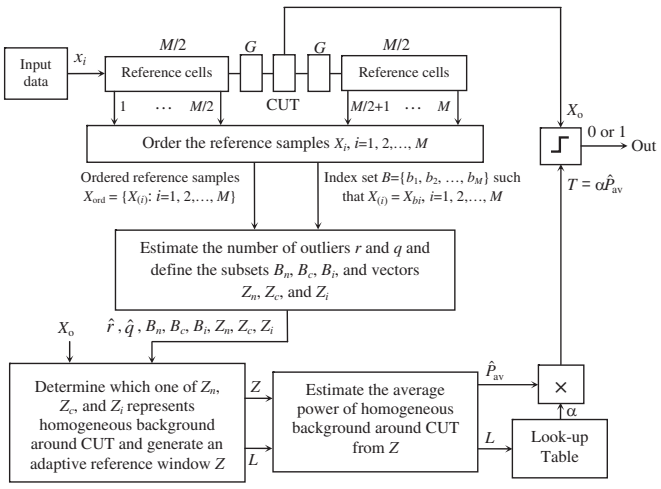

Figure 7. Possible implementations of adaptive OFPI-CFAR.

$(i = 1, 2, \ldots, N_r)$ are a succession of N_r samples of radar return signals, representing successive range cells in a scene or successive range cells and Doppler cells associated with each range cell if information on a scene is presented in the form of range-Doppler data matrix. Each of these return signals may be optionally the result of "within beam integration", whereby samples in each range or range-Doppler cell resulting from successive radar returns within the radar antenna dwell time are integrated.

In Figure 7, the CUT is at the center of a group of $M + 2G + 1$ cells, where G is the number of optional guard cells on either side of the CUT, the purpose of the guard cells being to avoid the spill-over of the target signal in the full reference window. The samples from $2G$ guard cells and the CUT sample X_o are not included in the full reference window, while the M samples from the reference cells represent the full reference window $X = \{X_1, X_2, \ldots, X_M\}$, where X_i are assumed to be independent random values, but not identically distributed when outliers are present, and the CUT sample X_o is assumed to be statistically independent with all X_i, $i = 1, 2, \ldots, M$.

The OFPI-CFAR detector in Figure 7 includes ordering procedure that generates a vector of reference samples sorted in ascending order according to their magnitudes $X_{ord} = [X_{(1)}, X_{(2)}, \ldots, X_{(M)}]$, $X_{(1)} \leq X_{(2)} \leq \ldots \leq X_{(M)}$, and a set of indices $B = \{b_1, b_2, \ldots, b_M\}$, which indicates the positions of the ordered samples in the full reference window before ordering, i.e., $X_{(i)} = X_{b_i}$, $1 \leq i \leq M$. To implement the ordering procedure the OFPI-CFAR detector can use any of widely known sorting algorithms [7], for example, so-called "quicksort" algorithm. These sorting algorithms are also known to provide an index set indicating the positions of sorted numbers in an initial unsorted array.

The vector X_{ord} and the set B are further used to estimate the number of outliers r and q in the full reference window and to retrieve from the set B the following subsets of indices ($\hat{r}$ and $\hat{q}$ stand for the estimates of r and q, respectively): a) $B_n = \{b_1, b_2, \ldots, b_{M-\hat{r}}\}$ that supposedly contains the indices (positions) of the reference samples in the region S_n; b) $B_c = \{b_{M-\hat{r}+1}, b_{M-\hat{r}+2}, \ldots, b_{M-\hat{q}}\}$ that supposedly contains the positions of the samples in the region S_c; c) $B_i = \{b_{M-\hat{q}+1}, b_{M-\hat{q}+2}, \ldots, b_M\}$ that supposedly represents the positions of the samples that belong to the S_i. The subsets B_n, B_c and B_i are used to generate the corresponding vectors Z_n, Z_c and Z_i from the vector X_{ord}. The vector Z_n of length $L_n = M - \hat{r}$ is determined as $Z_n = \{X_{(1)}, X_{(2)}, \ldots, X_{(M-\hat{r})}\}$, hence it supposedly represents the reference samples from the region S_n. The vector Z_c of length $L_c = \hat{r} - \hat{q}$ is determined as $Z_c = \{X_{(M-\hat{r}+1)}, X_{(M-\hat{r}+2)}, \ldots, X_{(M-\hat{q})}\}$, hence it supposedly represents the reference samples from the region S_c. The vector $Z_i = \{X_{(M-\hat{q}+1)}, X_{(M-\hat{q}+2)}, \ldots, X_{(M)}\}$ of length $L_i = \hat{q}$ supposedly represents the reference samples from the region S_i.

The CUT sample X_o, estimated number of outliers $\hat{r}$ and $\hat{q}$, and the subsets B_n, B_c and B_i are sent to the decision procedure for determining which of the vectors Z_n, Z_c and Z_i represents the homogeneous background in the vicinity of the CUT. After making a decision an adaptive reference window $Z = [Z_1, Z_2, \ldots, Z_L]$ is generated as that one of the vectors Z_n, Z_c and Z_i, which is declared to represent the homogeneous background around the CUT.

The adaptive detection threshold T is computed as $T = \alpha \hat{P}_{av}$, where $\hat{P}_{av}$ is an estimate of the average background power derived from the vector Z and α is the threshold multiplier (CFAR constant) extracted from a stored look-up table containing the values of the threshold multipliers which are precomputed for the predetermined false alarm probability P_{FA} as a function of the length of adaptive reference window L and in concordance with statistical distribution of the estimate of the average power derived from the adaptive reference window Z. A non-zero output detection signal is generated whenever $X_o \geq T$.

2.2. Estimating the Number of Outliers

Various approaches can be used for the purpose of estimating the number of outliers r and q that appear in the full reference window due to the clutter and interfering targets (see Figure 6). A straightforward way is to use the statistical hypothesis testing. This approach can be implemented by using the step-by-step censoring procedures introduced in [3] for the GTL-CMLD detector and in [5] for the generalized CMLD detector. Other attractive approach, proposed in [6] for estimating the number of interfering targets, is based on the information theoretic criteria principle. In the present paper, we use an estimation algorithm employing a step-by-step censoring procedure, which is similar to that suggested in [3, 5]. In contrast to [3, 5], where the censoring procedure uses the CA-CFAR principle, in

the present paper this procedure is based on the OS-CFAR principle. The algorithm for estimating the number of outliers is further referred to as (r, q)-estimation algorithm.

Figure 8 shows flow-chart of the (r, q)-estimation algorithm. As can be seen, this algorithm operates on the ordered sequence of the reference samples $X_{(1)} \leq X_{(2)} \leq \ldots \leq X_{(M)}$. Firstly, the algorithm estimates the total number of outliers r in the full reference window using the following step-by-step censoring procedure. At the m-th step of the censoring procedure, $m = 1, 2, \ldots, M-1$, the $(m+1)$-th ordered sample $X_{(m+1)}$ is compared against the censoring threshold $T_m = \beta_m X_{(Rm)}$, where β_m is the censoring threshold multiplier at the m-th step, $X_{(Rm)}$ is the R_m-th sample selected from the censoring reference window $X_{(1)}, X_{(2)}, \ldots, X_{(m+1)}$, and R_m is the representative sample rank at the m-th step. If for the first $m-1$ steps the adaptive censoring thresholds $T_i = \beta_i X_{(Ri)}$, $i = 1, 2, \ldots, m-1$ have not been exceeded and at the m-th step $X_{(m+1)} \geq T_m = \beta_m X_{(Rm)}$ then the total number of outliers is estimated as $\hat{r} = M - m$. It is clear that $\hat{r} = 0$ and $\hat{q} = 0$ when the procedure reaches the last step, i.e., $m = M-1$ and $X_{(M)} < T_{M-1}$. If $\hat{r} > 0$, the (r, q)-estimation algorithm proceeds to the estimation of q using as an input the vector $Y_{ord} = [Y_1, Y_2, \ldots, Y_{\hat{r}}]$, where $Y_i = X_{(m+i)}$, $i = 1, 2, \ldots, \hat{r}$, instead of the vector X_{ord} and the same censoring procedure. The number of outliers q is estimated as $\hat{q} = \hat{r} - k$, where k is that first integer at which $Y_{k+1} \geq \beta_k Y_{Rk}$, $k = 1, 2, \ldots, \hat{r} - 1$.

The subsets B_n, B_c, B_i and the vectors Z_n, Z_c, and Z_i are computed from the following equations

$$
\begin{array}{l}
if\ \hat{r} = 0 \\
\quad B_n = B, \quad B_c = \varnothing,\ B_i = \varnothing \\
\quad Z_n = X_{ord},\ Z_c = \varnothing,\ Z_i = \varnothing, \\
else \\
\quad \left[\begin{array}{l}
if\ \hat{q} = 0 \\
\quad B_n = \{b_1, \ldots, b_{M-\hat{r}}\}, \quad B_c = \{b_{M-\hat{r}+1}, \ldots, b_M\}, \quad B_i = \varnothing \\
\quad Z_n = \{X_{(1)}, \ldots, X_{(M-\hat{r})}\},\ Z_c = \{X_{(M-\hat{r}+1)}, \ldots, X_{(M)}\},\ Z_i = \varnothing \\
else \\
\quad B_n = \{b_1, \ldots, b_{M-\hat{r}}\}, \quad B_c = \{b_{M-\hat{r}+1}, \ldots, b_{M-\hat{q}}\}, \quad B_i = \{b_{M-\hat{q}+1}, \ldots, b_M\} \\
\quad Z_n = \{X_{(1)}, \ldots, X_{(M-\hat{r})}\},\ Z_c = \{X_{(M-\hat{r}+1)}, \ldots, X_{(M-\hat{q})}\},\ Z_i = \{X_{(M-\hat{q}+1)}, \ldots, X_{(M)}\} \\
end
\end{array} \right. \\
end
\end{array}
\tag{1}
$$

where the symbol $\varnothing$ stands for the empty set. The length (number of elements) of the vectors Z_n, Z_c, and Z_i is given by $L_n = M - \hat{r}$, $L_c = \hat{r} - \hat{q}$, and $L_i = \hat{q}$, respectively.

The censoring threshold multipliers β_m, $m = 1, 2, \ldots, M-1$ are precomputed as OS-CFAR constants for the predetermined probability of false censoring P_{fc} and corresponding values of R_m assuming homogeneous censoring reference window with exactly $m+1$ samples, i.e., assuming that the outliers are infinitely strong and X_{m+1} is the last outlier-free sample. This assumption has also been used in [5] for deriving the censoring threshold multipliers based on the CA-CFAR principle. The values of R_m, $m = 1, 2, \ldots, M-1$ are specified based on the optimum representative rank corresponding to the minimum of the average decision threshold (ADT) [8]. The ADT values are computed under the condition that the false alarm probability is equal to the probability of false censoring P_{fc}. Equation for computing the optimum representative rank is derived in Appendix A. The derivation of the censoring threshold multipliers β_m based on the OS-CFAR principle is given in Appendix B, where the values of R_m and corresponding values of β_m are summarized in Table B1 for $M = 32$, $P_{fc} = 10^{-3}$ and 10^{-4}.

2.3. Decision Strategy

To maintain robust false alarm and detection performance any adaptive CFAR detector has to identify the true homogeneous region in the vicinity of the CUT. Once such a region is determined, an adaptive reference window Z properly representing homogeneous background can be selected and, therefore, the robustness of CFAR performance is achieved.

The GTL-CMLD detector [3] uses the following decision strategy

$$
if\ \hat{r} < M/2 \rightarrow X_o \sim \hat{S}_n \quad else \rightarrow X_o \sim \hat{S}_c \tag{2}
$$

where $\hat{S}_n$ and $\hat{S}_c$ are the estimated clear and clutter regions, respectively, which are represented by the corresponding vectors Z_n and Z_c, and the notation $X \sim S$ reads as "X is in S" and means that the

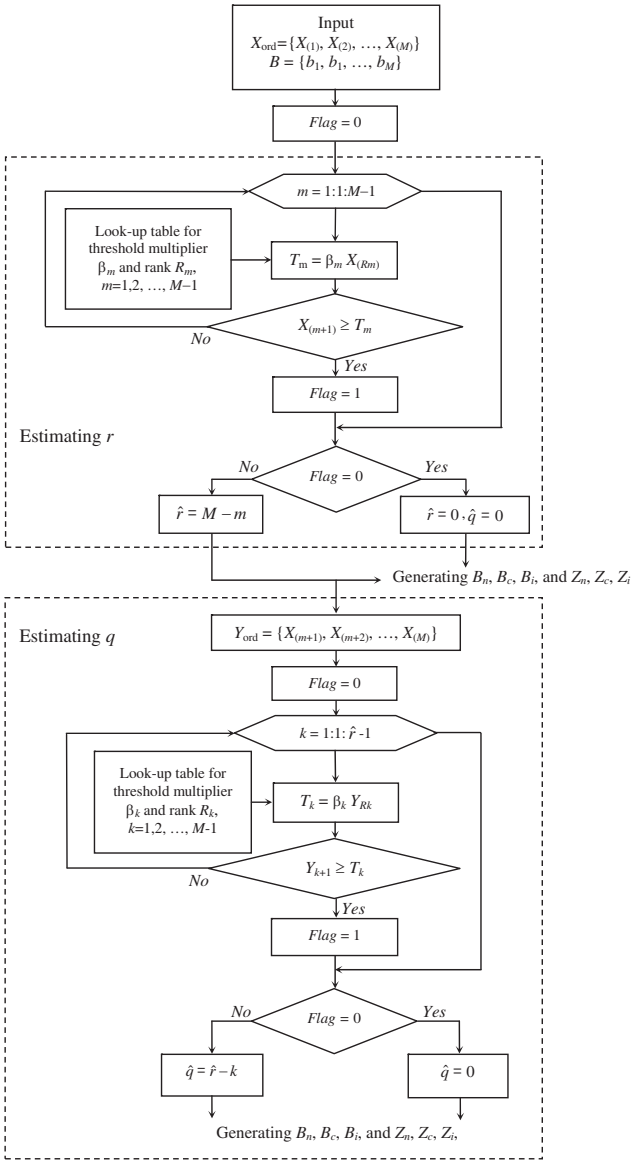

Figure 8. Flow-chart of the (r, q)-estimation algorithm.

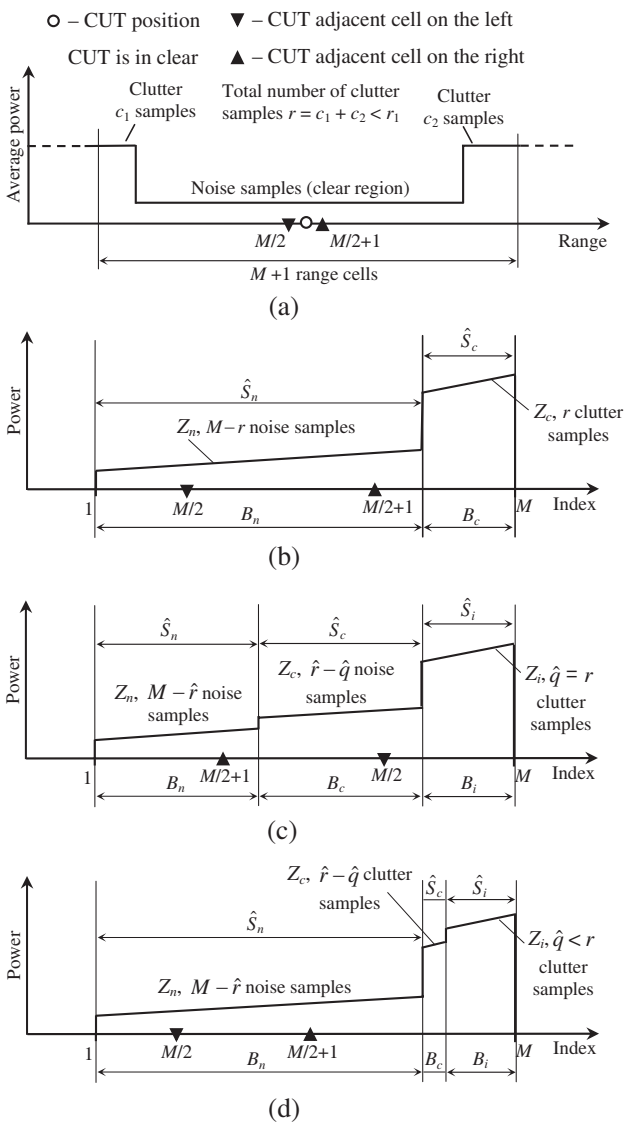

Figure 9. Clutter patch of a limited extent in the full reference window. (a) True number of clutter samples $r < r_1 < L^{cl}_{\min}$. (b) Reference samples after sorting, $\hat{r} = r$ and $\hat{q} = 0$. (c) Reference samples after sorting, $\hat{r} > r$ and $\hat{q} = r$. (d) Reference samples after sorting, $\hat{r} = r$ and $\hat{q} < r$.

distribution of a random variable X is supposedly identical to that of samples in a vector Z associated with the region S (the samples in Z are assumed to have identical distributions). Formula (2) represents the decision strategy from [3] in terms of the estimate $\hat{r}$; in [3] this strategy is formulated in terms of the index of the test m. The relationship between m and $\hat{r}$ is given by $m = M - \hat{r}$. As follows from (2) the decision strategy adopted in the GTL-CMLD detector is to declare $X_o \sim \hat{S}_n$ whenever $\hat{r} < M/2$ and $X_o \sim \hat{S}_c$ whenever $\hat{r} \geq M/2$. Declaring the CUT is in $\hat{S}_c$ for $\hat{r} = M/2$ is suggested in [3] in order to avoid the situation when excessive number of false alarms may result if the CUT is actually in clutter but it is declared to be in the clear. The decision strategy represented by formula (2) is further referred to as the CMLD-DS.

A critical issue for the GTL-CMLD detector based on the CMLD-DS is significant degradation in the false alarm regulation property for a clutter power transition with very large clutter-to-noise ratio CNR (CNR $\gg 1$) when $r \geq M/2$ (in this case the CUT resides in the clutter). To prove this we consider the scenario depicted in Figure 1, where $M = 32$ and $r = 20$. Since very large CNR is assumed, with probability one the clutter samples occupy the 20 top ranks after ordering. Obviously, because of false censoring the number of clutter samples in the full reference window is not always estimated correctly (since CNR $\gg 1$ errors caused by failure in clutter edge detection can be neglected). Let's assume that only one false censoring occurs when the censoring procedure runs for the noise samples occupying the lowest 12 ranks. Then, with some probability P_1 that is close to the probability of false censoring ($P_1 \approx P_{fc}$) the censoring procedure stops at some m ($1 \leq m \leq 11$), and we get $\hat{r} = M - m > 20$. Then, the procedure continues and with probability one (CNR $\gg 1$) the censoring procedure declares $\hat{q} = 20$. Therefore, we obtain the following three estimated regions $\hat{S}_n$, $\hat{S}_c$ and $\hat{S}_i$ represented by the vectors $Z_n = \{X_{(1)}, \ldots, X_{(m)}\}$, $Z_c = \{X_{(m+1)}, \ldots, X_{(12)}\}$ and $Z_i = \{X_{(13)}, \ldots, X_{(32)}\}$, respectively. These three estimated regions incorrectly represent the true homogeneous regions S_n and S_c represented by the vectors $Z_n = \{X_{(1)}, \ldots, X_{(12)}\}$ and $Z_c = \{X_{(13)}, \ldots, X_{(32)}\}$, respectively. As one can see, due to false censoring the true clear region S_n is incorrectly represented by the two estimated regions $\hat{S}_n$ and $\hat{S}_c$, while the true clutter region S_c is identified as $\hat{S}_i$. Since $\hat{r} > M/2 = 16$ the CMLD-DS declares that $X_o \sim \hat{S}_c$. The corresponding vector $Z_c = \{X_{(m+1)}, \ldots, X_{(12)}\}$ contains samples from the clear region S_n, hence, the CFAR threshold is incorrectly lowered and the corresponding conditional probability of false alarm $P_{fa1} \approx 1$ because the CUT is in clutter and CNR $\gg 1$.

If no false censoring occurs when the censoring procedure runs for the noise samples occupying the lowest 12 ranks the following two outcomes for the estimation results are possible: i) $\hat{r} = 20$ and $\hat{q} = 0$ in case of no false censoring when the censoring procedure tests the clutter samples, which occupy the top 20 ranks after sorting, and ii) $\hat{r} = 20$ and $\hat{q} = k <20$ if the false censoring occurs for the clutter samples with probability P_3, where $P_3 \approx P_{fc}$. For the case i), we have correctly estimated homogeneous regions $\hat{S}_n = S_n$ and $\hat{S}_c = S_c$. Hence, the threshold is properly computed from the clutter samples and the corresponding conditional probability of false alarm P_{fa2} is equal to the design probability of false alarm, $P_{fa2} = P_{FA}$. For the case ii), we have three estimated regions represented by the vectors $Z_n = \{X_{(1)}, \ldots, X_{(12)}\}$, $Z_c = \{X_{(13)}, \ldots, X_{(M-k)}\}$ and $Z_i = \{X_{(M-k+1)}, \ldots, X_{(32)}\}$, respectively. In this case the vector Z_c contains a subset of clutter samples from the true region S_c, hence, the CFAR threshold is properly estimated and the corresponding conditional probability of false alarm $P_{fa3} = P_{FA}$. Taking into account that no false censoring occurs with probability $P_2 = 1 - P_1 - P_3 \approx 1 - 2P_{fc}$ and using the law of total probability yields for the overall probability of false alarm P_{FA}^o

$$P_{FA}^o = P_1 \times P_{fa1} + P_2 \times P_{fa2} + P_3 \times P_{fa3} \approx P_{fc} + (1 - 2P_{fc}) \cdot P_{FA} + P_{fc} \cdot P_{FA}.$$

As follows from this equation, $P_{FA}^o \approx P_{fc}$ when $P_{FA} \ll P_{fc}$, i.e., the overall probability of false alarm P_{FA}^o increases significantly with respect to the design value P_{FA}. For instance, assuming $P_{fc} = 10^{-4}$ and $P_{FA} = 10^{-6}$ yields $P_{FA}^o \approx 10^{-4} + 0.9998 \cdot 10^{-6} + 10^{-4} \cdot 10^{-6} \approx 10^{-4} \gg 10^{-6}$. Thus, the false alarm regulation property of the CMLD-DS significantly degrades, especially if $P_{FA} \ll P_{fc}$, in the presence of clutter edge when CNR $\gg 1$, $r \geq M/2$ and the CUT is in clutter.

The CMLD-DS decision strategy, which is used by GTL-CMLD detector, does not employ any detailed information on the positions of the outlier-free reference samples. As discussed previously, ignoring this information may result in serious performance degradation (see also Subsection 3.2). In contrast to the GTL-CMLD detector, this information is essentially employed by the OFPI-CFAR methods.

This subsection is not intended to derive a kind of optimum decision strategy to be used in the OFPI-CFAR for identifying the true homogeneous regions in the full reference window. Rather, it illustrates some possible ways of using the sample in the test cell and information provided by the estimates $\hat{r}$, $\hat{q}$ and the subsets B_n, B_c, and B_i in order to define such a decision strategy that ensures the robustness of the OFPI-CFAR performance in spite of inevitable errors in estimating the number

$$
\begin{array}{l}
1\,[if\ \hat{r} < r_1 \rightarrow X_o \sim \hat{S}_n \\
\ else\ if\ \hat{r} \geq r_2 \\
\quad 2\ \left[\begin{array}{l} if\ \hat{q} = 0 \rightarrow X_o \sim \hat{S}_c \\ else \\ \quad 3\ \left[\begin{array}{l} if\ X_o \leq Z_n(L_n)\ and\ [(M/2) \in B_n\ or\ (M/2+1) \in B_n] \rightarrow\ X_o \sim \hat{S}_n \\ else \\ \quad 4\ \left[\begin{array}{l} if (M/2) \in B_n\ and\ (M/2+1) \in B_n \rightarrow X_o \sim \hat{S}_n \\ else\ if [(M/2) \in B_n\ and\ (M/2+1) \in B_i] \\ \qquad or\ [(M/2) \in B_i\ and\ (M/2+1) \in B_n] \rightarrow X_o \sim \hat{S}_n \\ else\ if (M/2) \in B_c\ or\ (M/2+1) \in B_c \rightarrow X_o \sim \hat{S}_c \\ else \rightarrow X_o \sim \hat{S}_i \\ end \end{array}\right. \\ end \end{array}\right. \\
\ else \\
\quad 5\ \left[\begin{array}{l} if\ X_o \leq Z_n(L_n)\ and\ [(M/2) \in B_n\ or\ (M/2+1) \in B_n] \rightarrow\ X_o \sim \hat{S}_n \\ else \\ \quad 6\ \left[\begin{array}{l} if (M/2) \in B_n\ and\ (M/2+1) \in B_n \rightarrow X_o \sim \hat{S}_n \\ else\ if [(M/2) \in B_n\ and\ (M/2+1) \in B_i] \\ \qquad or\ [(M/2) \in B_i\ and\ (M/2+1) \in B_n] \rightarrow X_o \sim \hat{S}_n \\ else\ if (M/2) \in B_c\ or\ (M/2+1) \in B_c \rightarrow X_o \sim \hat{S}_c \\ else \rightarrow X_o \sim \hat{S}_i \\ end \end{array}\right. \\ end \end{array}\right. \\
end
\end{array}
\tag{3}
$$

of outliers. It is clear that any reasonable decision strategy has to aim for maximizing the probability of correct decision on which one of the estimated homogeneous regions adequately represents the true homogeneous background around the CUT. In this paper we propose one of the reasonable decision strategies, which is given by a set of rules presented in formula (3), where r_1 and r_2 are fixed integers. The decision strategy given by formula (3) is further referred to as the OFPI-DS. Having decided which one of the estimated regions $\hat{S}_n$, $\hat{S}_c$ or $\hat{S}_i$ represents the homogeneous background around the CUT the adaptive reference vector Z of length L is readily determined using the following rule

$$
\begin{array}{l}
if\ X_o \sim \hat{S}_n \rightarrow Z = Z_n,\ L = L_n = M - \hat{r} \\
if\ X_o \sim \hat{S}_c \rightarrow Z = Z_c,\ L = L_c = \hat{r} - \hat{q} \\
if\ X_o \sim \hat{S}_i \rightarrow Z = Z_i,\ L = L_i = \hat{q}
\end{array}
\tag{4}
$$

Including in formula (3) the rule $X_o \leq Z_n(L)$, which uses the CUT sample X_o, is motivated by the following reason. Strictly speaking, the estimates $\hat{r}$, $\hat{q}$ and the subsets B_n, B_c, and B_i do not contain information that explicitly indicates whether or not the CUT sample X_o is in $\hat{S}_n$. To increase the probability of correct decisions on which one of the estimated regions adequately represents the true homogeneous background around the CUT it is reasonable to use information that directly indicates whether $X_o \sim \hat{S}_n$ or $X_o \notin \hat{S}_n$. Such information can be obtained simply by performing statistical hypothesis test used in the (r, q)-estimation algorithm

$$
if\ X_o < \beta_m X_{(R_m)} \rightarrow X_o \sim \hat{S}_n \quad else\ X_o \notin \hat{S}_n \tag{5}
$$

where m, β_m, and R_m correspond to the m-th step at which $X_{(m+1)} \geq \beta_m X_{(Rm)}$ when the (r, q)-estimation algorithm estimates the total number of outliers r. Other simple way is to use the following test

$$
if\ X_o \leq Z_n(L_n) \rightarrow\ X_o \sim \hat{S}_n \quad else\ X_o \notin \hat{S}_n \tag{6}
$$

where $Z_n(L_n) = \max(Z_n)$ is the maximum element in Z_n. The rule given by (6) is stronger than that given by (5) because $Z_n(L_n) < \beta_m X_{(Rm)}$. The rule from Equation (6) is included in the OFPI-DS decision strategy given by formula (3).

In this paper, the OFPI-DS is designed heuristically by analyzing several typical scenarios (those depicted in Figures 1–5 and some additional scenarios) with the purpose of finding such a set of decision rules that properly identifies the homogeneous region around the CUT even if the number of outliers is estimated incorrectly. Our design assumes that the parameters r_1 and r_2 can be set within the following limits $0 \le r_1 \le M/2$ and $M/2 \le r_2 \le M$. As shown in Subsection 3.2, the rationale for using the parameter r_1 in (3) is that setting r_1 closer to its lower limit provides significant reduction in the false alarm rate with respect to that of the CMLD-DS in case of extended clutter edge with moderate CNR level (about 10 dB) when the number of clutter samples $r > M/2$. It is also shown that setting the parameter r_2 closer to M allows the OFPI-CFAR detector to maintain robust detection performance in multiple target environments even if the number of outliers due to interferers is greater than $M/2$. Our heuristic design also assumes that the clutter-to-noise ratio CNR $\gg 1$, the interfering target-to-noise ratio INR $\gg$ CNR, and only one false censoring can occur during the censoring procedure.

In Appendix C, our design of the OFPI-DS is illustrated with an additional example. In this Section we discuss the OFPI-DS for the case of limited clutter extent shown in Figure 9(a). According to formula (3), whenever $\hat{r} < r_1$, the OFPI-DS always declares that the CUT is in $\hat{S}_n$ without taking into account the information in the subset B_n. The rationale for this decision is to allow the primary target to be reliably detected in the presence of closely spaced neighboring targets with no risk of increasing the false alarm probability. This rule can be confirmed based on the following physically justified assumption: the extent of a continuous clutter patch is limited from below by some value $L^{cl}_{\min} < M/2$ that is the minimum clutter extension in range expressed in the number of samples, for example $L^{cl}_{\min} = M/4+1$. This means that even when the whole clutter patch entirely resides in the full reference window there must be present at least $L^{cl}_{\min}$ clutter outliers. Let's assume that r_1 meets the inequality $r_1 < L^{cl}_{\min} = M/4 + 1$ and the true number of clutter outliers in the full reference window is $r < r_1$ and no interfering targets are present. Since the clutter extent $r < r_1 < L^{cl}_{\min}$ the only situation when the clutter occupies $r < L^{cl}_{\min}$ cells is shown in Figure 9(a) where the number of clutter cells c_1 and c_2 meet the conditions $0 \le c_1 \le r$, $0 \le c_2 \le r$, $c_1 + c_2 = r < r_1$.

Figure 9(b) shows the estimated homogeneous regions $\hat{S}_n$, $\hat{S}_c$ and $\hat{S}_i$ along with corresponding subsets B_n, B_c, B_i and vectors Z_n, Z_c and Z_i for the case when the number of outliers is correctly estimated. Figure 9(c) and Figure 9(d) represent similar data for the cases when the number of outliers is incorrectly estimated due to false censoring. Analyzing Figure 9(b), when $\hat{r} = r < r_1$ and $\hat{q} = 0$, yields that according to the rule $if\, \hat{r} < r_1 \rightarrow\ X_o \sim \hat{S}_n$ as predefined by formula (3), the vector Z_n is selected as the adaptive reference vector Z, i.e., $Z = Z_n$. Since Z_n exactly represents the homogeneous background around the CUT the OFPI-CFAR threshold is properly computed (CUT is in the clear) and the conditional false alarm probability corresponding to this case is equal to the design probability of false alarm P_{FA}. Consider the case shown in Figure 9(c), when $\hat{r} > r$ and $\hat{q} = r$. Obviously, if $\hat{r} < r_1$ then again $Z = Z_n$ and the corresponding conditional false alarm probability is equal to the design P_{FA}. If $\hat{r} \ge r_1$ then according to formula (3) irrespective of which one is true, $r_1 \le \hat{r} < r_2$ or $\hat{r} \ge r_2$, only the following two decisions are possible: 1) $Z = Z_n$ when both of the indices $M/2$ and $M/2+1$ are in the subset B_n, i.e., $M/2 \in B_n$ and $M/2+1 \in B_n$, and 2) $Z = Z_c$ because when $M/2 \notin B_n$ or $M/2+1 \notin B_n$ then at least one of these indices is in B_c because with probability one the integers $M/2$ and $M/2+1$ belong to the sum of subsets B_n and B_c. Since each of the vectors Z_n and Z_c contains only noise samples the OFPI-CFAR threshold is properly computed and the corresponding conditional false alarm probability is equal to P_{FA}. Analyzing Figure 9(d) readily shows that in this case the only decision $Z = Z_n$ is possible because $\hat{r} = r < r_1$; therefore, the corresponding conditional false alarm probability is equal to P_{FA}.

Combining the results of analysis for scenario shown in Figure 9(a) in terms of the law of total probability one can conclude that the overall false alarm probability is equal to the design P_{FA}. Thus, in this scenario the false alarm performance of the OFPI-CFAR based on the OFPI-DS given by formula (3) remains robust even in the presence of errors in estimating the number of outliers.

2.4. Adaptive CFAR Threshold

The adaptive CFAR threshold is computed as $T = \alpha \hat{P}_{av}$, where α is the threshold multiplier (CFAR constant), which is precomputed for the predetermined false alarm probability P_{FA}, and $\hat{P}_{av}$ is an estimate of the average background power around the CUT. The precomputed threshold multipliers are extracted from the stored look-up table accordingly to the length L of the adaptive reference window Z (see Figure 7).

The OFPI-CFAR estimates the average power $\hat{P}_{av}$ from the adaptive reference window Z (see Figure 7), which supposedly represents the homogeneous background in the vicinity of the CUT. Recall that Z is defined according to formula (4) after taking decision on which one of the estimated regions $\hat{S}_n$, $\hat{S}_c$ or $\hat{S}_i$ represents this homogeneous background. At least two methods can be used to estimate $\hat{P}_{av}$. The method suggested in [3, 5] is based on the CA-CFAR principle, i.e., $\hat{P}_{av}$ is computed by using a sum of all the samples in Z. The present paper considers a procedure based on the OS-CFAR principle. To compute $\hat{P}_{av}$ the procedure extracts from a stored look-up table the precomputed value of the representative rank K corresponding to L, $1 \le L \le M$, and then extracts the K-th ordered sample Z_K from the adaptive reference window $Z = \{Z_1, Z_2, \ldots, Z_K, \ldots, Z_L\}$. As known from the OS-CFAR theory [8, 9] Z_K can be treated as an estimate of the average background power, i.e., $\hat{P}_{av} = Z_K$, under assumption that the reference window is homogeneous. In this paper the value of K is precomputed for each $L = 1, 2, \ldots, M$ as an integer that minimizes the average decision threshold (ADT) according to the definition in [8]. Equations for computing the optimum K and corresponding OS CFAR constant α are derived in Appendix A; for $M = 32$, numerical results are summarized in Table A1 at $P_{FA} = 10^{-4}$ and 10^{-6}.

3. PERFORMANCE ANALYSIS

In this Section we study the false alarm and detection performance of the adaptive OFPI-CFAR that employs the OFPI-DS decision strategy given by formula (3). To evaluate the performance improvement we also compare the OFPI-CFAR with the GTL-CMLD detector that uses the CMLD-DS given by formula (2).

In this study we assume that the input data x_i (Figure 7) represent a sequence of independent random values resulted from noncoherent integration of N independent samples taken at the output of a square-law detector for every range cell. Both the noise and clutter samples are assumed to obey zero-mean Gaussian distribution at the input of a square-law detector. Hence, at the output of the square-law detector both the noise and clutter samples are governed by an exponential distribution. The statistical independence of clutter samples before noncoherent integration is merely assumed in our analysis for the sake of simplicity. However, this assumption is reasonable, for example, in radar systems employing frequency agility and/or time diversity in order to circumvent the deep fade of return echo on a single transmission which results in poor system performance [1]. To simplify the performance analysis we also assume the Swerling II fluctuation model for both the primary target and interfering targets. Recall that for this model the N target samples at the output of the square-law detector are independent identically distributed random variables governed by an exponential distribution.

Under these assumptions each sample x_i obeys a gamma distribution as a result of noncoherent integration of N independent exponentially distributed samples. Hence, the probability density function (PDF) $p(x)$ and the cumulative distribution function (CDF) $P(x)$ of x_i are given by

$$p(x) = D^N \frac{x^{N-1}}{(N-1)!} \exp(-Dx), \quad x \ge 0 \tag{7}$$

$$P(x) = 1 - \exp(-Dx) \sum_{k=0}^{N-1} \frac{(Dx)^k}{k!}, \quad x \ge 0 \tag{8}$$

The parameter of the distribution D depends on the contents of the range cell associated with x_i. If the range cell contains noise alone $D = 1/(2\sigma^2)$, where σ^2 is the variance of noise. If the range cell contains clutter $D = 1/[2\sigma^2(1+\mathrm{CNR})]$, with CNR being the clutter-to-noise power ratio at the input of

the square-law detector. For the range cells containing interfering targets $D = 1/[2\sigma^2(1 + \text{INR})]$, with INR being the interfering target-to-noise power ratio at the input of the square-law detector. When the range cells contain both the clutter and interfering targets $D = 1/[2\sigma^2(1+\text{CNR}+\text{INR})]$ since the radar returns due to clutter and interfering or primary targets are assumed to be statistically independent. When the primary target is present in the CUT then $D = 1/[2\sigma^2(1 + \text{SNR})]$, where SNR is the signal-to-noise ratio at the input of the square-law detector. Therefore, for the CUT the parameter D can be specified according to the following formula

$$D = \begin{cases} 1/[2\sigma^2(1 + \text{SNR})] & \text{for clear background} \\ 1/[2\sigma^2(1 + \text{CNR} + \text{SNR})] & \text{for clutter background} \end{cases} \tag{9}$$

where SNR = 0 if the CUT contains noise alone or noise plus clutter, and SNR > 0 if the primary target is assumed to be present. Without loss of generality we assume $2\sigma^2 = 1$.

3.1. Simulation Procedure

Explicit equations for the false alarm and detection performance of the adaptive OFPI-CFAR are difficult to derive because they require knowledge of the PDF $p_T(x)$ of the adaptive threshold T. Unfortunately, we have not found any closed-form expression of this PDF for both the OFPI-CFAR and the GTL-CMLD detector. Examining the principle of operation of the proposed adaptive OFPI-CFAR implementation shows that the distribution of T is given by a finite mixture distribution. The partial distributions of the mixture are the distributions of the k-th order statistics that are randomly selected according to the OFPI-DS decision strategy from a group of M non-identically distributed reference samples. The derivation of a closed-form equation for the PDF $p_T(x)$ is a complicated problem because these order statistics are conditioned by the selection of the adaptive reference window, which is in an intricate nonlinear dependence on the decision making process. In order to circumvent this difficulty, we have resorted to statistical simulations using a version of Monte-Carlo method described in Appendix D in terms of the false alarm probability P_{FA} estimation. However, the method is not restricted to the estimation of P_{FA} since it can be equally well used to estimate the detection probability after appropriate substitution for the CDF of the CUT sample.

In the course of simulations we compute the relative standard deviation STD γ (see Appendix D) of the Monte-Carlo estimator and compare γ with required value $\gamma_{req} = 10\%$. If $\gamma \geq \gamma_{req}$ the number of trials N_{is} is doubled, then a new set of statistically independent random samples $T_1, T_2, \ldots, T_{N_{is}}$ is generated and the estimation procedure is repeated until the condition $\gamma < \gamma_{req}$ is met. In estimating the false alarm performance $N_{is} = 8000$ is used as an initial setting when the estimated false alarm probability is greater than or equal to 10^{-6}. When the estimated P_{FA} is less than 10^{-6} and in situations when the problem of gross bias error may occur (see Appendix D) the simulations are carried out with initial setting $N_{is} = 10^5$. If the current number of trials N_{is} exceeds $N_{is\text{Max}} = 800000$ the estimation procedure is terminated irrespective of the achieved STD value γ. To estimate the probability of detection the initial setting $N_{is} = 2000$ and $N_{is\text{Max}} = 2000$ are used in all scenarios related to the evaluation of the detection performance.

Throughout the simulations the number of reference samples is set at $M = 32$ and the number of noncoherently integrated samples is set at $N = 6$ for all cases.

The precomputed values of the optimum ranks K and corresponding threshold multipliers α for both of the GTL-CMLD and OFPI-CFAR detectors are taken from Table A1 in Appendix A. The censoring procedure is implemented using the precomputed values of R_m and β_m, $m = 1, 2, \ldots, M-1$ from Table B1 in Appendix B.

3.2. Numerical Results

In Figure 10 we compare the false alarm regulation property of the proposed version of the OFPI-CFAR (denoted by OFPI-DS) and that of the GTL-CMLD detector (denoted by CMLD-DS) versus the true number of clutter samples r when one clutter edge with CNR $\gg 1$ is present in the full reference window. It is assumed that the design probability of false alarm and false censoring is $P_{FA} = 10^{-4}$ and $P_{fc} = 10^{-3}$, respectively, for the noise distribution $D = 1$ and the clutter-to-noise ratio CNR = 20 dB, and $r_1 = 9$, $r_2 = 22 > M/2$ for the OFPI-DS. For $r \geq M/2 = 16$ the simulations are carried out

with initial setting $N_{is} = 10^5$. The plots in Figure 10 clearly demonstrate an essential advantage of the OFPI-DS. It is seen that the OFPI-DS maintains the false alarm probability at the specified design value independently on r, while the CMLD-DS seriously fails for $r \geq M/2 = 16$. The CMLD-DS curve in Figure 10 confirms our analysis in Subsection 2.3, where we prove that for $P_{FA} \ll P_{fc}$ the false alarm regulation property of the CMLD-DS significantly degrades in the presence of a region of clutter power transition with CNR $\gg 1$ when $r \geq M/2$ and the CUT resides in the clutter.

Figures 11 and 12 compare the false alarm performance of the OFPI-DS and that of the CMLD-DS in the presence of one clutter edge at CNR = 5 and 10 dB, respectively, as a function of the true number of clutter samples r assuming $P_{FA} = 10^{-4}$, $P_{fc} = 10^{-4}$, and $r_1 = 9$, $r_2 = M/2 = 16$ for the OFPI-DS. The simulations are carried out using initial setting $N_{is} = 10^5$ at point $r = M/2 = 16$. Analyzing these figures yields that for relatively small value of the CNR (about 5 dB) the false alarm performance for both of the CFAR approaches are quite similar while for moderate CNR (about 10 dB) the false alarm

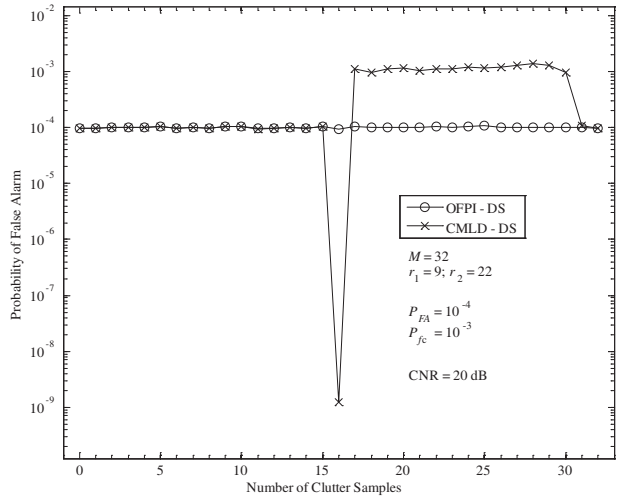

Figure 10. Probability of false alarm in clutter power transition at CNR = 20 dB, $r_1 = 9$, $r_2 = 22 > M/2$; design $P_{FA} = 10^{-4}$, $P_{fc} = 10^{-3}$.

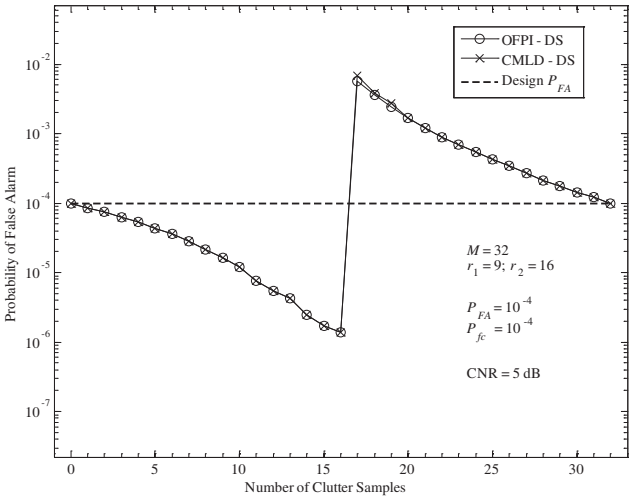

Figure 11. Probability of false alarm in clutter power transition at CNR = 5 dB, $r_1 = 9$, $r_2 = M/2 = 16$; design $P_{FA} = 10^{-4}$, $P_{fc} = 10^{-4}$.

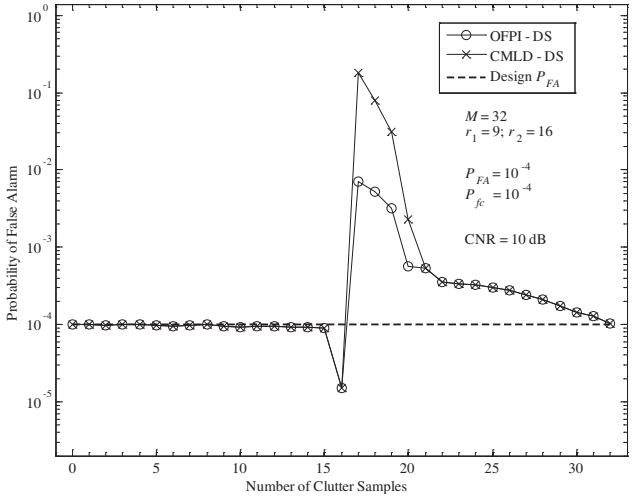

Figure 12. Probability of false alarm in clutter power transition at CNR = 10 dB, $r_1 = 9$, $r_2 = M/2 = 16$; design $P_{FA} = 10^{-4}$, $P_{fc} = 10^{-4}$.

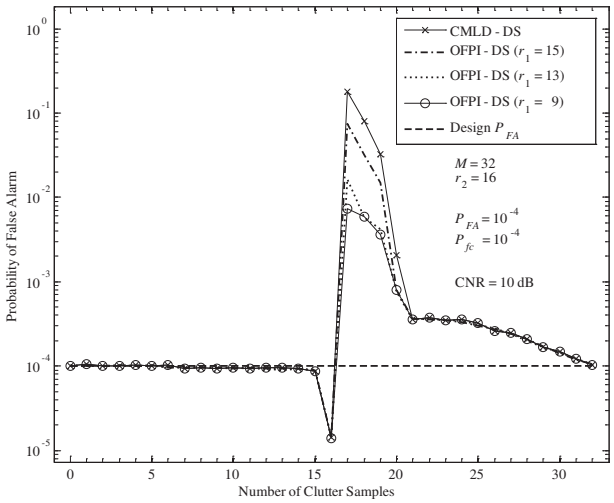

Figure 13. Effect of r_1 on false alarm performance at fixed r_2; CNR = 10 dB, $P_{FA} = 10^{-4}$, $P_{fc} = 10^{-4}$.

regulation property of the OFPI-DS is evidently superior to that of the CMLD-DS.

Figure 13 shows the effect of r_1 ($r_1 = 9, 13, 15$) at fixed $r_2 = M/2 = 16$ and Figure 14 shows the effect of r_2 ($r_2 = 16, 20, 24$) at fixed $r_1 = 9$ on the false alarm performance of the OFPI-DS depending on the true number of clutter samples r in case of one clutter edge for CNR = 10 dB, $P_{FA} = 10^{-4}$, $P_{fc} = 10^{-4}$. At point $r = M/2 = 16$ the simulation is carried out with initial setting $N_{is} = 10^5$. The false alarm performance of the CMLD-DS does not depend on r_1 and r_2 and is merely plotted here for the purpose of comparison. From Figure 13, it is seen that decreasing r_1 from 15 to 9 significantly reduces the false alarm probability for the OFPI-DS with respect to that of the CMLD-DS within the interval $17 \leq r \leq 20$.

For the CMLD-DS, the relatively high level of false alarm rate within the interval $17 \leq r \leq 20$, when the CUT is in the clutter, can be explained as follows. For moderate CNR, the (r, q)-estimation algorithm relatively frequently underestimates the number of outliers, so that for $17 \leq r \leq 20$ the probability of the event $\hat{r} < M/2$ is relatively high especially when r is close to $M/2 + 1$. Therefore, the CMLD-DS, which takes decisions based on the inequality $\hat{r} < M/2$, relatively frequently selects improper adaptive reference window that contains all the noise samples and only some small part of the clutter samples. Thus, the adaptive detection threshold is unacceptably lowered and the false alarm probability is increased. When r increases the probability of the event $\hat{r} < M/2$ decreases, so that the CMLD-DS properly estimates the detection threshold more frequently and the false alarm probability gradually decreases to the specified design value P_{FA}. In contrast to the CMLD-DS, the OFPI-DS uses additional information that results in increasing the probability of correct decisions on the selection of the adaptive reference window. For the OFPI-DS, improvement in the false alarm regulation property is especially prominent when the parameter r_1 is set at a lower level. Using low values of r_1 results in extending the lower portion of the interval $[r_1, r_2)$ of possible values for $\hat{r}$, within which the OFPI-DS can compensate the underestimation errors due to its enhanced capability to take correct decisions. This confirms that the reasonable choice for r_1 is to define it based on the minimum clutter extension in range $r_1 = L^{cl}_{\min} < M/2$, as discussed in Subsection 2.3.

The plots in Figure 14 show that increasing r_2 for the OFPI-DS leads to extending the interval for the true number of outliers (for $r \geq 17$), within which the false alarm probability remains nearly some constant level. Nevertheless, this level does not exceed the maximum value at a point $r = M/2+1 = 17$ when the setting $r_2 = M/2 = 16$ is used. Such behavior of the OFPI-DS curves depending on r_2 is caused by extending the upper portion of the interval $[r_1, r_2)$. This extending leads to increasing the

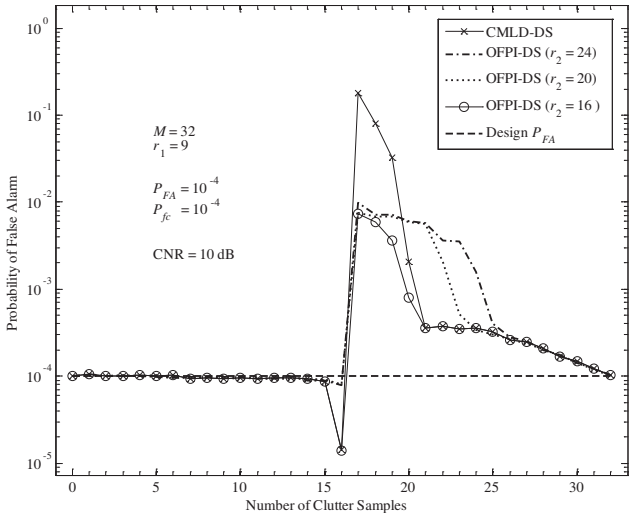

Figure 14. Effect of r_2 on false alarm performance at fixed r_1; CNR = 10 dB, $P_{FA} = 10^{-4}$, $P_{fc} = 10^{-4}$.

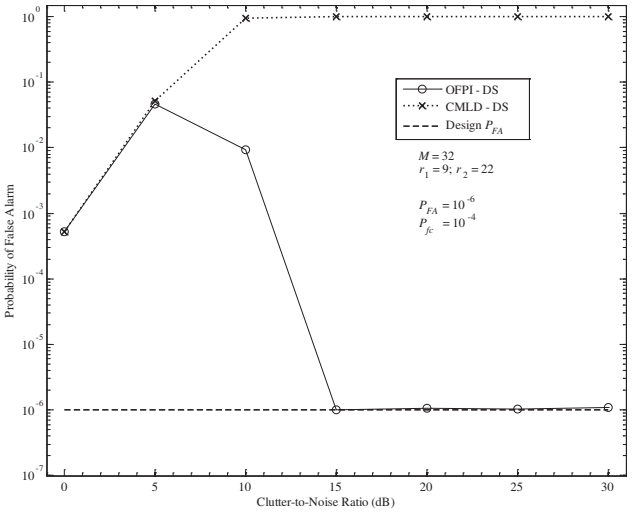

Figure 15. Probability of false alarm versus CNR when CUT and adjacent cells are in clutter $r = 12$ clutter samples; $r_1 = 9$, $r_2 = 22$; design $P_{FA} = 10^{-6}$, $P_{fc} = 10^{-4}$.

probability that the decisions are taken through the chain of rules marked in formula (3) by numbers 5-6 and decreasing the probability that the chain 2-3-4 is used for taking decisions. For the chain 5-6 the probability of declaring that $X_o \sim \hat{S}_n$ is higher than that for the chain 2-3-4. Thus, the maximum level of the false alarm probability at point $r = 17$ extends within the interval $[M/2+1,\, r_2)$. The simulations for CNR ≥ 15 dB have shown that the false alarm performance of the OFPI-DS with $M/2 < r_2 < M$ and $r_1 < M/2$ does not depend on r_2 and is very similar to that plotted in Figure 10. It is shown further (see Figure 18) that using large values of r_2 results in essentially robust detection performance of the OFPI-DS in multiple target environments even when the number of outliers exceeds $M/2$.

Figure 15 demonstrates the clear superiority of the OFPI-DS over the CMLD-DS in terms of the false alarm regulation property in scenario shown in Figure 4(a), where $r+1 = 13$ clutter samples occupy the cells from 14 to 26, therefore, the CUT and its two adjacent samples are in the clutter. The curves in these figures are plotted against the clutter-to-noise ratio CNR at the design $P_{FA} = 10^{-6}$, $P_{fc} = 10^{-4}$, and using the setting $r_1 = 9$ and $r_2 = 22$ for the OFPI-DS. For CNR ≥ 15 dB the simulations are carried out with initial setting $N_{is} = 10^5$. From Figure 15, it is seen that for CNR ≥ 15 dB the false alarm probability for the OFPI-DS is very close to the design value P_{FA}, while for the CMLD-DS the false alarm probability intolerable increases starting from CNR = 10 dB.

Figure 16 compares the false alarm regulation property of the OFPI-DS and CMLD-DS in scenario shown in Figure 4(a), when the CUT moves through the clutter patch consisting of $r + 1 = 13$ clutter samples. The false alarm probability is computed for $P_{FA} = 10^{-6}$ and CNR = 15 dB and plotted against the distance d expressed as the number of range cells between the CUT and leading edge of the clutter patch. For points $d = -12, -11, \ldots, 0, 1$, the simulations are carried out with initial setting $N_{is} = 10^5$. From Figure 16, the definite advantage of the OFPI-DS over the CMLD-DS is evident.

We now turn to the detection performance evaluation. In Figure 17 the detection probability is plotted as a function of the primary target SNR for scenarios shown in Figure 3(a) and Figure 5(a), where 20 clutter samples occupy the cells $1, 2, \ldots, 10$ and $23, 24, \ldots, 32$ in the full reference window. The graphs in Figure 17 are plotted for two cases: when no interfering targets are present, i.e., $r = 20$, $q = 0$, and when $q = 10$ samples due to the interfering targets are in the clutter. The clear superiority of the OFPI-DS over the CMLD-DS is evident from Figure 17.

Next, we analyze the detection performance in scenario depicted in Figure 2, where the primary target is to be detected in multiple target environments. In Figure 18 the probability of detection is plotted versus the number of outliers q due to interfering targets; for the OFPI-DS the parameter r_1 is fixed ($r_1 = 9$) and the parameter r_2 is sequentially set at 18, 22, and 26. It is seen in Figure 18 that a

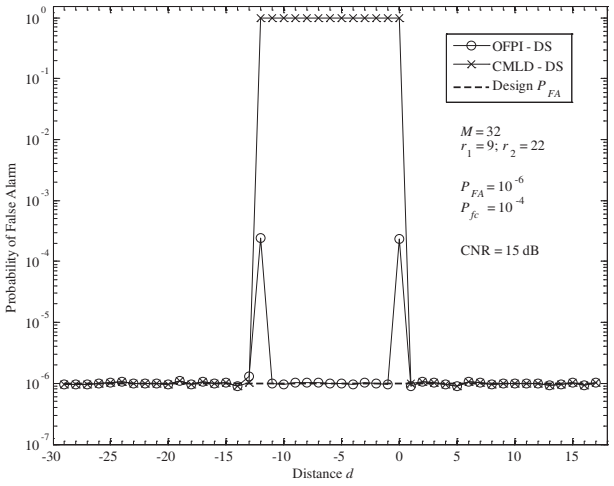

Figure 16. Probability of false alarm versus the distance d for CNR = 15 dB, $r = 12$ clutter samples; $r_1 = 9$, $r_2 = 22$; design $P_{FA} = 10^{-6}$, $P_{fc} = 10^{-4}$.

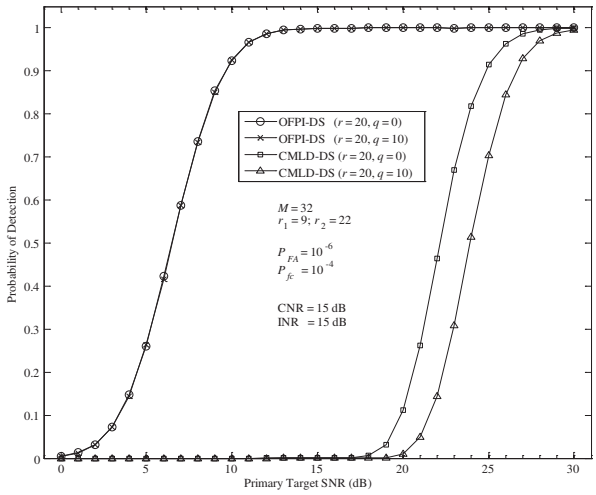

Figure 17. Probability of detection versus SNR for primary target at CNR = 15 dB and INR = 15 dB, $r_1 = 9$, $r_2 = 22$; design $P_{FA} = 10^{-6}$, $P_{fc} = 10^{-4}$.

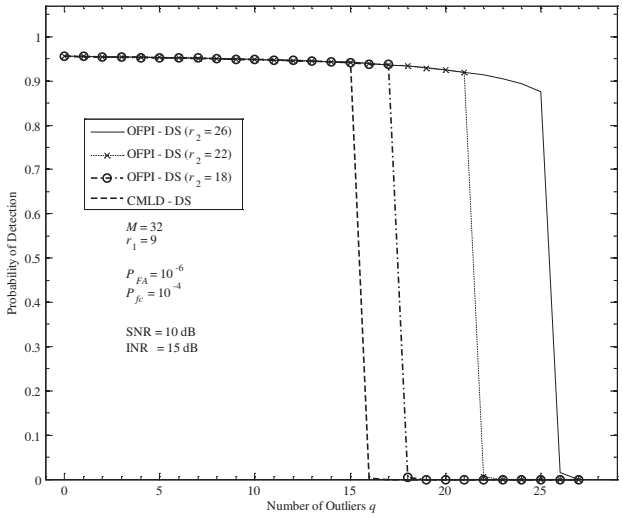

Figure 18. Probability of detection versus number of outliers q ($r = q$) for SNR = 10 dB and INR = 15 dB; $r_1 = 9$ fixed, $r_2 = 18$, 22, and 26; design $P_{FA} = 10^{-6}$, $P_{fc} = 10^{-4}$.

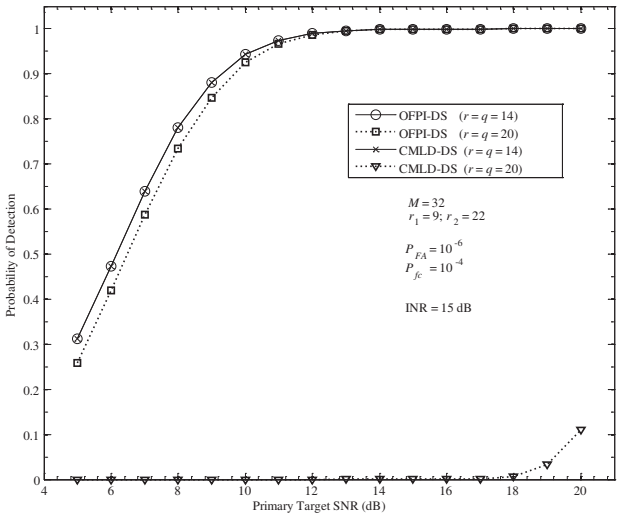

Figure 19. Probability of detection versus SNR for primary target at $q = 14$ and 20; $r_1 = 9$, $r_2 = 22$; design $P_{FA} = 10^{-6}$, $P_{fc} = 10^{-4}$, INR = 15 dB.

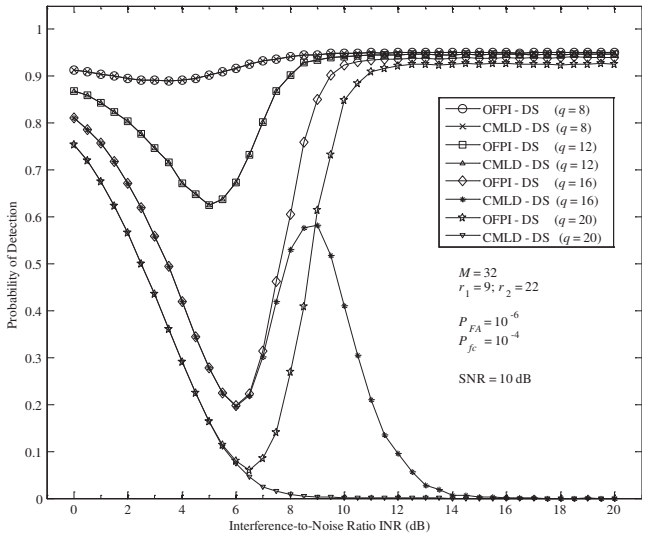

Figure 20. Probability of detection versus INR for $q = 8, 12, 16$, and 20 ($r = q$); $r_1 = 9$, $r_2 = 22$; design $P_{FA} = 10^{-6}$, $P_{fc} = 10^{-4}$, SNR = 10 dB.

remarkable feature of the OFPI-DS is its ability to maintain essentially robust detection performance even when the number of outliers exceeds $M/2$, i.e., $q > M/2$. As expected, the CMLD-DS detector collapses when $q \geq M/2$.

The simulation results in Figure 19 and Figure 20 correspond to scenario shown in Figure 2. In Figure 19 the estimated detection probability P_D is plotted versus the primary target SNR and in Figure 20 the P_D is plotted versus the interfering target-to-noise ratio (INR) for the fixed primary target SNR = 10 dB. The graphs in Figure 19 are computed at $q = 14, 20$ ($r = q$) and in Figure 20 at $q = 8, 12, 16$, and 20 ($r = q$). From these figures, when $q < M/2 = 16$ the detection performances of the CMLD-DS and the OFPI-DS are identical and demonstrate good target detection ability of these methods. However, when $q \geq M/2$ the CMLD-DS collapses, while the OFPI-DS is able to maintain reliable target detection.

4. CONCLUSIONS

In this paper, a new class of adaptive CFAR methods intended for achieving robust performance in the presence of clutter edges and interfering targets has been proposed. This class of CFAR methods is referred to as the OFPI-CFAR. A fundamental distinction of the OFPI-CFAR methods is that in order to maintain robust false alarm and detection performance these methods essentially use information on positions at which estimated outlier-free samples appear in the full reference window and the statistics of the sample in the cell under test. This information and the magnitude of the sample in the test cell are used by a decision procedure, which attempts to identify such a subset of reference samples that most adequately represent homogeneous background around the test cell.

One version of the OFPI-CFAR based on a heuristically designed decision strategy has been suggested in the present paper. The performance of this version has been evaluated and compared with that of the well-known GTL-CMLD detector. It has been shown through statistical simulations that the suggested OFPI-CFAR is superior to the GTL-CMLD detector in the false alarm regulation property and target detection performance in nonhomogeneous environments.

The results of simulations have shown that in the presence of one clutter edge with CNR $\gg 1$ the suggested OFPI-CFAR is able to perfectly maintain the false alarm rate at the specified design level independently on the number of clutter cells in the full reference window, while the CMLD-DS seriously fails in regulating the false alarm rate when the number of clutter cells exceeds half of the number of reference samples. The proposed OFPI-CFAR has also demonstrated the clear superiority over the GTL-CMLD in terms of the false alarm regulation property in situations with two clutter edges. For example, when clutter patch of a limited extent, which does not exceed half of the number of reference samples, is present in the full reference window and CNR ≥ 15 dB the false alarm rate for the OFPI-CFAR is maintained at the specified design level, while for the GTL-CMLD the false alarm rate intolerably increases.

It has also been shown that the OFPI-CFAR exhibits excellent detection performance in multiple target environments. In particular, the attractive feature of the proposed OFPI-CFAR is its ability to maintain essentially robust detection performance even when the number of outliers due to interfering targets exceeds half of the number of reference samples, whereas the GTL-CMLD detector fails drastically.

In conclusion, it should be stated that using information on the positions, at which outlier-free samples appear in the full reference window, and the statistics of the test cell can be regarded as one of the basic CFAR principles for achieving essentially robust performance in nonhomogeneous environments. This principle can be used for designing of various modifications of adaptive OFPI-CFAR algorithms for a wide range of practical applications in which the outliers due to clutter edges and interfering targets can be present.

ACKNOWLEDGMENT

This work is sponsored by Institute for Information and Communications Technology Promotion, Ministry of Science, ICT and Future Planning of South Korea, under ICT R&D Program [R0101-15-0066, Small (SSPA 200W level) X-band Dual Polarization Weather Radar System Development for Localized Disaster Prevention].

APPENDIX A. COMPUTING OPTIMUM REPRESENTATIVE RANK AND OS-CFAR CONSTANT TO BE USED IN DETERMINING ADAPTIVE DETECTION THRESHOLD

In this appendix we compute the optimum representative rank K and the corresponding OS-CFAR constant to be used in determining the adaptive detection threshold T, which is computed as $T = \alpha Z_K$, where α is the OS-CFAR constant and Z_K is the K-th ordered sample Z_K from the adaptive reference window $Z = [Z_1, Z_2, \ldots, Z_K, \ldots, Z_L]$ of length L. The OS-CFAR constant α is precomputed for the predetermined design P_{FA} as a function of $L = 1, 2, \ldots, M$, and in accordance with statistical distribution of the K-th order statistic in homogeneous reference window of length L. For each L the

rank K is defined as an optimum value corresponding to the minimum of the average decision threshold (ADT) [8].

At first, we present the computation of the optimum rank K. Since we consider the homogeneous reference window without loss of generality we can assume $D = 1$ for the gamma distribution given by formulae (7) and (8). Then, according to [8] the ADT corresponding to the K-th order statistic in a reference window of length L is defined as the normalized quantity

$$ADT_{L,K} = \alpha_{L,K} E\left(Z_K\right) \tag{A1}$$

where $L = 1, 2, \ldots, M-1$, $K = 1, 2, \ldots, L$; $\alpha_{L,K}$ is the OS-CFAR constant computed for to the specified P_{FA} at fixed L and K; Z_K is the K-th order statistic, and E denotes the expectation. The optimum K as a function of L is determined by minimizing $ADT_{L,K}$

$$K_{opt}(L) = \arg\min_{K}(ADT_{L,K}) \tag{A2}$$

To obtain equation for computing the scalar factors $\alpha_{L,K}$ let's consider the following definition for the probability of false alarm P_{FA}

$$P_{FA} = \int_0^\infty \left[1 - P_{CUT}(\alpha_{L,K} x)\right] p_{(K)}(x, L) dx \tag{A3}$$

where $P_{CUT}(x)$ is the CDF of the CUT under hypothesis H_o (no target) and $p_{(K)}(x, L)$ is the PDF of the K-th order statistic out of L independent and identically distributed continuous random variables with CDF $P(x)$ and PDF $p(x)$

$$p_{(K)}(x, L) = K \left(\begin{array}{c} L \\ K \end{array} \right) \left[P(x)\right]^{K-1} \left[1 - P(x)\right]^{L-K} p(x) \tag{A4}$$

Substituting $p(x)$ from Equation (7), $P(x)$ and $P_{CUT}(x)$ from Equation (8) with setting $D = 1$ into Equations (A4) and (A3) yields the following formula that has been earlier derived in [9, Eq. (49)]

$$\begin{aligned} P_{FA} \;=\; & K \left(\begin{array}{c} L \\ K \end{array} \right) \int_0^\infty \left[\exp(-\alpha_{L,K} x) \sum_{i=0}^{N-1} \frac{(\alpha_{L,K} x)^i}{i!} \right] \times \left[1 - \exp(-x) \sum_{i=0}^{N-1} \frac{x^i}{i!} \right]^{K-1} \\ & \times \left[\exp(-x) \sum_{i=0}^{N-1} \frac{x^i}{i!} \right]^{L-K} \frac{x^{N-1} \exp(-x)}{(N-1)!} dx \end{aligned} \tag{A5}$$

The right hand side of Equation (A5) has to be integrated numerically. For given P_{FA} we compute the scalar factors $\alpha_{L,K}$ using (A5) iteratively.

By definition, $E(Z_K)$ is the first non-central moment

$$E\left(Z_K\right) = \int_0^\infty x\, p_{(K)}(x, L) dx \tag{A6}$$

Substituting, as before, $p(x)$ and $P(x)$ given by Equations (7) and (8) with $D = 1$ into (A4) we get from (A6) the following formula for computing $E(Z_K)$ using numerical integration

$$E\left(Z_K\right) = K \left(\begin{array}{c} L \\ K \end{array} \right) \int_0^\infty x \left[1 - \exp(-x) \sum_{i=0}^{N-1} \frac{x^i}{i!} \right]^{K-1} \left[\exp(-x) \sum_{i=0}^{N-1} \frac{x^i}{i!} \right]^{L-K} \frac{x^{N-1} \exp(-x)}{(N-1)!} dx \tag{A7}$$

In Figure A1, the average decision threshold $ADT_{L,K}$ is plotted as a function of the representative rank K for $M = 32$ and $P_{FA} = 10^{-6}$ at $L = 2, 4, \ldots 30, 32$.

For $M = 32$, $P_{FA} = 10^{-4}$ and 10^{-6} the optimum values of K and corresponding OS-CFAR constants α are given in Table A1. This table represents the basic format of the look-up table that is used in the adaptive OFSI-CFAR detector (Figure 7) for computing the adaptive OFSI-CFAR threshold $T = \alpha Z_K$. The value of optimum rank K and α is read from the cell corresponding to the predetermined P_{FA} and the estimated length L of the adaptive reference window.

Table A1. Optimum rank K and corresponding OS-CFAR constant α.

L	P_{FA}			
	10^{-4}		10^{-6}	
	K	α	K	α
1	1	11.1442823	1	26.0693626
2	2	5.1914721	2	8.9223852
3	3	3.9299157	3	6.1689768
4	4	3.3739879	4	5.0767136
5	4	3.8451512	4	5.6949706
6	5	3.4691186	5	5.0198216
7	6	3.2184007	6	4.5876164
8	6	3.4931202	6	4.9417629
9	7	3.2915020	7	4.6098990
10	8	3.1366208	8	4.3603625
11	8	3.3319728	8	4.6112447
12	9	3.1979785	9	4.4013758
13	9	3.3572233	10	4.2307620
14	10	3.2395649	10	4.4257936
15	11	3.1403217	11	4.2752819
16	11	3.2695820	12	4.1472464
17	12	3.1796234	12	4.3070564
18	13	3.1012287	13	4.1908250
19	13	3.2100844	14	4.0889997
20	14	3.1375825	14	4.2244911
21	15	3.0729787	15	4.1303024
22	15	3.1670306	16	4.0460768
23	16	3.1064601	16	4.1637359
24	17	3.0516102	17	4.0847993
25	17	3.1344218	17	4.1913629
26	18	3.0824881	18	4.1171470
27	19	3.0348816	19	4.0493398
28	19	3.1088638	19	4.1445889
29	20	3.0634546	20	4.0802817
30	20	3.1316690	21	4.0209270
31	21	3.0882902	21	4.1070480
32	22	3.0479753	22	4.0503807

APPENDIX B. COMPUTING THRESHOLD MULTIPLIERS FOR CENSORING PROCEDURE

This Appendix derives equation for computing the censoring threshold multipliers to be used in the censoring procedure that is an essential part of the (r, q)-algorithm for the estimating the number of outliers in the full reference window.

As discussed in Subsection 2.2, the (r, q)-algorithm operates on the ordered sequence of the reference samples $X_{(1)} \leq X_{(2)} \leq \ldots \leq X_{(M)}$ and at the m-th step of the censoring procedure, $m = 1, 2, \ldots, M-1$,

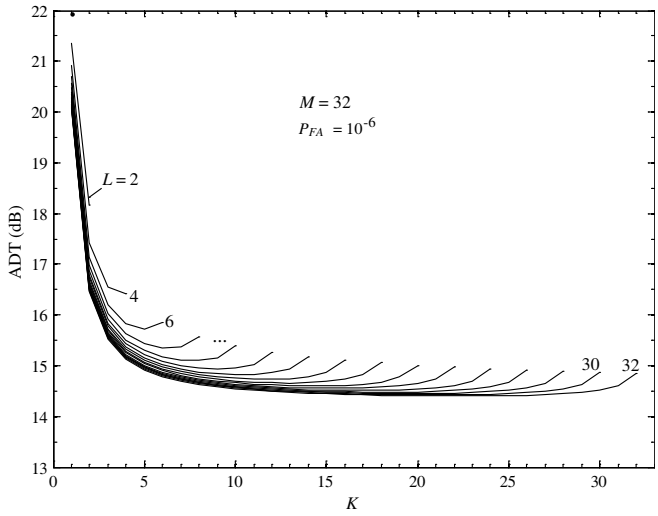

Figure A1. ADT versus representative rank K at different L for $M = 32$ and $P_{FA} = 10^{-6}$

the $(m+1)$-th ordered sample $X_{(m+1)}$ is compared against the censoring threshold $T_m = \beta_m X_{(Rm)}$, where β_m is the censoring threshold multiplier at the m-th step, $X_{(Rm)}$ is the R_m-th sample selected from the censoring reference window $X_{(1)}, X_{(2)}, \ldots, X_{(m+1)}$, and R_m is the representative sample rank at the m-th step.

According to the approach we follow in the present paper the β_m, $m = 1, 2, \ldots, M-1$ are precomputed as OS-CFAR constants for the predetermined probability of false censoring P_{fc} and corresponding values of the representative rank R_m. In computing β_m we assume that $X_{(1)}, X_{(2)}, \ldots, X_{(m+1)}$ originate from the $m+1$ independent samples X_i representing homogeneous background and the remaining $M-m-1$ samples in the full reference window are due to infinitely strong outliers. Hence, $X_{(m+1)}$ is the last outlier-free sample. The probability of false censoring P_{fc} is the probability of making wrong decision at the m-th step on the condition that the censoring procedure reaches the m-th step

$$P_{fc} = \Pr\left(X_{(m+1)} \geq \beta_m X_{(R_m)} | X_{(i+1)} < \beta_i X_{(R_i)}, \quad i = 1, 2, \ldots, m-1\right) \tag{B1}$$

Under the above assumption P_{fc} can be represented as

$$P_{fc} = \int_0^\infty \int_{\beta_m x}^\infty p_{(R_m)(m+1)}(x, y)\, dydx \tag{B2}$$

where $p_{(R_m)(m+1)}(x, y)$ is the joint PDF of the R_m-th and $(m+1)$-th order statistics, $1 \leq R_m < m+1$ in the homogeneous censoring window of length $m+1$, $m = 1, 2, \ldots, M-1$.

To derive a closed-form equation for P_{fc} we consider a general expression for the joint PDF of the R-th and S-th order statistics generated from M independent and identically distributed random values X_i. This general expression is given by [10]

$$p_{(R)(S)}(x, y) = \frac{M!}{(R-1)!(S-R-1)!(M-S)!} P^{R-1}(x) p(x) \times [P(y) - P(x)]^{S-R-1} p(y) [1 - P(y)]^{M-S}$$
$$1 \leq R < S \leq M, \;\; x \leq y \tag{B3}$$

where $P(x)$ and $p(x)$ denotes the CDF and PDF of X_i, respectively.

Assuming $S = M$, i.e., S is always defined to be equal to M, we get from (B3)

$$p_{(R)(S)}(x, y) = \frac{S!}{(R-1)!(S-R-1)!} P^{R-1}(x) p(x) [P(y) - P(x)]^{S-R-1} p(y)$$
$$1 \leq R < S, \;\; x \leq y \tag{B4}$$

Setting $R = R_m$ and $S = m+1$ in Equation (B4) yields the following representation for P_{fc} in Equation (B2)

$$P_{fc} = c_1 \int_0^{\infty} \int_{\beta_m x}^{\infty} P^{R_m-1}(x)p(x)\left[P(y) - P(x)\right]^{m-R_m} p(y)dydx$$
$$x \le y,\ c_1 = (m+1)!/[(R_m-1)!(m-R_m)!],\ 1 \le R_m < m+1 \tag{B5}$$

Making in Equation (B5) the substitutions $u = P(x)$ and $v = P(y)$ yields

$$P_{fc} = c_1 \int_0^1 \int_a^1 [v-u]^{m-R_m} dv u^{R_m-1} du,\ a = P[\beta_m P^{-1}(u)] \tag{B6}$$

The inner integral in Equation (B6) is simply

$$\int_a^1 [v-u]^{m-R_m} dv = \left.\frac{(v-u)^{(m-R_m+1)}}{m-R_m+1}\right|_a^1 = \frac{1}{m-R_m+1}\left[(1-u)^{m-R_m+1} - (a-u)^{m-R_m+1}\right] \tag{B7}$$

Substituting Equation (B7) into Equation (B6) and turning back to the argument x yields

$$P_{fc} = c\int_0^{\infty} \left\{[1-P(x)]^{m-R_m+1} - [P(\beta_m x) - P(x)]^{m-R_m+1}\right\}\ [P(x)]^{R_m-1}\, p(x)dx$$
$$c = R_m \frac{(m+1)!}{R_m!\ (m+1-R_m)!},\ 1 \le R_m < m+1 \tag{B8}$$

Thus, using Equation (B8) for the distribution specified by Equations (7) and (8) the censoring constants β_m, $m = 1, 2, \ldots, M-1$ can be computed iteratively for the specified P_{fc} and R_m from

$$P_{fc} = c\int_0^{\infty} \left\{[Q(x)]^{m-R_m+1} - [Q(x) - Q(\beta_m x)]^{m-R_m+1}\right\}\ [P(x)]^{R_m-1}\, p(x)dx$$
$$c = R_m \frac{(m+1)!}{R_m!\ (m+1-R_m)!},\ 1 \le R_m < m+1 \tag{B9a}$$

or

$$P_{fc} = c\int_0^{\infty} \left\{[Q(x)]^{S-R_m} - [Q(x) - Q(\beta_m x)]^{S-R_m}\right\}\ [P(x)]^{R_m-1}\, p(x)dx$$
$$c = R_m \frac{S!}{R_m!\ (S-R_m)!},\quad 1 \le R_m < S,\ S = m+1 \tag{B9b}$$

where

$$Q(x) = \exp(-Dx)\sum_{k=0}^{N-1} \frac{(Dx)^k}{k!},\ x \ge 0 \tag{B10}$$

$$P(x) = 1 - \exp(-Dx)\sum_{k=0}^{N-1} \frac{(Dx)^k}{k!},\ x \ge 0 \tag{B11}$$

$$p(x) = D^N \frac{x^{N-1}}{(N-1)!}\exp(-Dx),\ x \ge 0 \tag{B12}$$

The censoring procedure suggested in the present paper possesses CFAR property in homogeneous background. To prove this it suffices to show that P_{fc} given by (B9) does not depend on the power of

homogeneous background. The proof readily follows from (B9) using the substitution $y = Dx$. So, in computing β_m we use the setting $D = 1$.

The value of R_m to be used in computing β_m is specified as $R_m = m$, for $m = 1, 2, 3$ and $R_m = K_{m+1}$, for $m = 4, 5, \ldots, M-1$, where K_m is the optimum representative rank computed as described in Appendix A for the probability of false alarm P_{FA} that is equal to the specified probability of false censoring P_{fc}. For $M = 32, P_{fc} = 10^{-3}$ and 10^{-4} the values of R_m and corresponding OS-CFAR constants β_m are given in Table B1. This table represents the basic format of the look-up table that is used in the censoring procedure (see Figure 8). The values of R_m and β_m are read from the cell corresponding to the step index m, $m = 1, 2, \ldots, M-1$, and specified P_{fc}.

Table B1. Optimum rank R and constant β for censoring procedure.

m	P_{fc}			
	10^{-3}		10^{-4}	
	R	β	R	β
1	1	8.0908442	1	12.7304287
2	2	4.4214940	2	5.9604211
3	3	3.5431964	3	4.5491714
4	4	3.1412344	4	3.9365087
5	5	2.9060557	5	3.5884402
6	5	3.3547122	6	3.3608418
7	6	3.1540599	6	3.8205051
8	7	3.0086222	7	3.6197772
9	7	3.2903523	8	3.4678102
10	8	3.1604650	8	3.7651880
11	9	3.0570035	9	3.6277099
12	9	3.2645779	9	3.8620894
13	10	3.1694176	10	3.7380822
14	11	3.0895393	11	3.6344821
15	11	3.2546461	11	3.8205087
16	12	3.1798072	12	3.7247710
17	13	3.1148708	13	3.6419663
18	13	3.2523072	13	3.7965963
19	14	3.1907141	14	3.7188613
20	14	3.3123474	15	3.6500168
21	15	3.2539563	15	3.7825451
22	16	3.2016466	16	3.7172070
23	16	3.3078361	17	3.6583412
24	17	3.2578149	17	3.7744331
25	18	3.2123585	18	3.7181208
26	18	3.3066747	19	3.6667249
27	19	3.2629285	19	3.7700963
28	20	3.2227333	20	3.7206354
29	20	3.3076265	20	3.8158655
30	21	3.2687538	21	3.7682567
31	22	3.2327216	22	3.7241662

APPENDIX C. AN ADDITIONAL EXAMPLE TO ILLUSTRATE DESIGN OF THE OFPI-DS

In this Appendix our heuristic design of the OFPI-DS decision strategy given by formula (3) is illustrated with an example in addition to that discussed in Subsection 2.3. This additional example addresses the detection performance of the OFPI-CFAR when the primary target is to be detected near the clutter edge in the presence of interfering targets. An example of this scenario is shown in Figure C1(a), where the full reference window of length $M = 32$ contains $r = 12$ outliers due to clutter and two groups of outliers (4 samples per group) due to interfering targets. Thus, the total number of outliers is $r = 20$ including $q = 8$ outliers due to interfering targets. It is assumed that the following setting is used for the OFPI-DS: $r_1 = 9$ and $r_2 = 22$.

From Figures C1(b) and (d) representing the cases when $\hat{r} = r = 20$, it is seen that the OFPI-DS always takes the decision $Z = Z_n$ (only noise samples) since in any event with probability one the index $M/2 = 16$ belongs to the subset B_n and the index $M/2 + 1 = 17$ belongs to B_i. For the case shown in Figure C1(c), when $\hat{r} = 26 > r_2 = 22$, the only two decisions are possible: 1) $Z = Z_n$ when $16 \in B_n$,

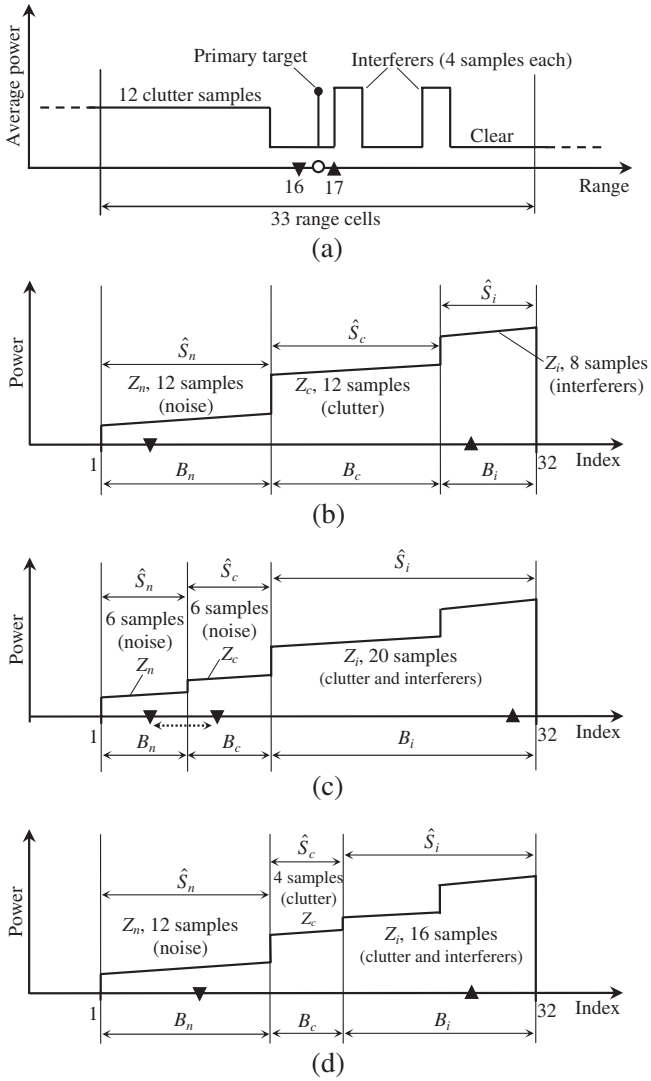

Figure C1. Detecting target near clutter edge in the presence of interfering targets. (a) Target near clutter edge and interfering targets. (b) Reference samples after sorting, $\hat{r} = r = 20$ and $\hat{q} = q = 8$. (c) Reference samples after sorting, $\hat{r} = 26$ and $\hat{q} = 20$. (d) Reference samples after sorting, $\hat{r} = 20$ and $\hat{q} = 16$.

and 2) $Z = Z_c$ when $16 \in B_c$; in either case the adaptive reference window Z contains noise samples. In Figures C1(c) the dotted double arrow between the black triangles indicates that the position (index) marked by the triangle appears only in one of the subsets where the triangle is placed (B_n or B_c) but not simultaneously in both of them.

As follows from formula (3), if the estimated number of outliers $\hat{r}$ were less than r_2 ($20 < \hat{r} < r_2 = 22$), the OFPI-DS would take exactly the same decisions. Combining the results of this analysis in terms of the law of total probability readily yields that the OFPI-CFAR detection performance remains robust in scenario shown in Figure C1(a).

APPENDIX D. ESTIMATING PROBABILITY OF FALSE ALARM

The method proposed in this Appendix for estimating the false alarm probability is based on using the knowledge of the distribution of the CUT sample: the CDF of the CUT sample is assumed to be given by Equation (8). This fact allows computing the probability of the CUT exceeding any given adaptive threshold. Thus, if we carry out N_{is} Monte-Carlo trials, and therefore generate a set of adaptive thresholds $T_1, T_2, \ldots, T_{N_{is}}$ (for each of the CFAR methods in question), the estimated probability of false alarm is given by the following unbiased Monte-Carlo estimator

$$\hat{P}_{FA} = \frac{1}{N_{is}} \sum_{k=1}^{N_{is}} \Pr\{X_o > T_k\} = \frac{1}{N_{is}} \sum_{k=1}^{N_{is}} G(T_k, D_{CUT}) \tag{D1}$$

where $G(x, D_{CUT}) = 1 - P(x, D_{CUT})$, with $P(x, D_{CUT})$ being the CDF of the CUT sample X_o given by Equation (8), where the parameter D is substituted with $D_{CUT} = 1$ if the CUT contains noise alone or with $D_{CUT} = 1/(1 + \mathrm{CNR})$ if the CUT contains noise plus clutter.

The sample variance of the estimator (D1) is given by

$$Var\{\hat{P}_{FA}\} = \frac{1}{N_{is}} \left(\frac{1}{N_{is}} \sum_{k=1}^{N_{is}} [G(T_k, D_{CUT})]^2 - [\hat{P}_{FA}]^2 \right) \tag{D2}$$

In the course of estimation procedure we compute the relative standard deviation STD γ using the estimate given by Equation (D1) and the sample variance given by Equation (D2) as

$$\gamma = \sqrt{Var\{\hat{P}_{FA}\}} / \hat{P}_{FA} \tag{D3}$$

and compare computed value of γ against a required value $\gamma_{req} = 10\%$. If $\gamma \geq \gamma_{req}$ the number of trials N_{is} is doubled, then a new set of statistically independent random samples $T_1, T_2, \ldots, T_{N_{is}}$ is generated and the estimation procedure is repeated until such a number of trials N_{is}^{fin} (final number of trials) is reached at which the condition $\gamma < \gamma_{req}$ is met for the first time.

It should be noted that the problem of gross bias error may occur in estimating false alarm probability for the adaptive CFAR methods even if N_{is} is defined from the condition $\gamma < \gamma_{req}$. This problem arises from the fact that the distribution of the adaptive CFAR threshold is inherently a finite mixture distribution with unknown weighting coefficients. Some terms in this mixture distribution have relatively small weighting coefficients which values are on the order of the probability of false censoring P_{fc} and lower. The weighting coefficients represent the probabilities with which corresponding terms appear in the mixture. If the conditional probability of false alarm associated with one of such terms is close to unity then the contribution of this term into the overall probability of false alarm may become dominant. An example when the problem of gross bias error may occur is discussed in Subsection 2.3. That example proves that the GTL-CMLD [3] may suffer significant degradation of false alarm performance in case of clutter power transition with CNR $\gg 1$ when $r \geq M/2$ and the CUT is in the clutter.

If the number of independent statistical trials N_{is} is on the order of or less than $1/P_{fc}$, then the terms making significant contribution into the overall probability of false alarm may insufficiently be represented in the sequence of independent random samples $T_1, T_2, \ldots, T_{N_{is}}$ that simulate the adaptive threshold T. The shortage of statistically significant terms results in an estimate of the false alarm probability, which is significantly different from that when they appear in the sequence

$T_1, T_2, \ldots, T_{N_{is}}$ in sufficient quantity. However, even though these two estimates may differ significantly their corresponding γ may simultaneously meet the condition $\gamma < \gamma_{req}$. This is possible because γ characterizes the precision of the Monte-Carlo estimator (D1) taking into account only those components of the mixture distribution of the adaptive CFAR threshold T that are actually present in the sequence $T_1, T_2, \ldots, T_{N_{is}}$.

To illustrate the problem of gross bias error we consider scenario shown in Figure 1 assuming that $r = 20$ and the clutter-to-noise ratio CNR = 25 dB. Table D1 compares the $\hat{P}_{FA}$ estimates obtained for the CFAR methods under study at $M = 32$, $r_1 = 9$, $r_2 = 22$, $P_{FA} = 10^{-4}$, $P_{fc} = 10^{-4}$ and $\gamma_{req} = 10\%$ using initial settings $N_{is} = 1000$ and 100000.

From Table D1, it is seen that for the GTL-CMLD algorithm the relative difference between the $\hat{P}_{FA}$ estimates obtained with initial settings $N_{is} = 1000$ ($N_{is}^{fin} = 1000$) and 100000 ($N_{is}^{fin} = 400000$) is 93.43%, while their γ meet the condition $\gamma < 10\%$. However, one can assume that only the estimate obtained with $N_{is} = 100000$ ($N_{is}^{fin} = 400000$) is free of the gross bias error because in this case the estimator (D1) takes into account, with high probability, considerably greater number of the mixture components that make principal contributions into the overall probability of false alarm. For the OFPI-CFAR, the $\hat{P}_{FA}$ estimates obtained simultaneously with the corresponding estimates for the GTL-CMLD are very close (relative difference is 1.54%), so one can assume that both of these estimates are free of the gross bias error.

Table D1. Illustration of gross bias error by comparing false alarm probability estimates.

CFAR Method	N_{is}	N_{is}^{fin}	$\hat{P}_{FA}$	γ (%)
GTL-CMLD	1000	1000	1.01546×10^{-4}	8.51
	100000	400000	1.94974×10^{-4}	7.91
OFPI-CFAR	1000	1000	1.01546×10^{-4}	8.51
	100000	400000	1.00002×10^{-4}	0.42

REFERENCES

1. Richards, M. A., et al., *Principles of Modern Radar, Vol. I: Basic Principles*, Chapter 16, SciTech, Raleigh, NC, 2010.
2. Gandhi, P. P. and S. A. Kassam, "Analysis of CFAR processors in nonhomogeneous background," *IEEE Transactions on Aerospace and Electronic Systems*, Vol. 24, No. 4, 427–445, Jul. 1988.
3. Himonas, S. D. and M. Barkat, "Automatic censored CFAR detection for nonhomogeneous environments," *IEEE Transactions on Aerospace and Electronic Systems*, 286–304, Vol. 28, No. 1, Jan. 1992.
4. Pourmottaghi, A., M. R. Taban, and S. Gazor, "A CFAR detector in a nonhomogeneous weibull clutter," *IEEE Transactions on Aerospace and Electronic Systems*, Vol. 48, No. 2, 1747–1758, Apr. 2012.
5. Barkat, M., S. D. Himonas, and P. K. Varshney, "CFAR detection for multiple target situations," *IEE Proceedings*, Vol. 136, Pt. F, No. 5, 193–209, Oct. 1989.
6. Magaz, B., A. Belouchrani, and M. Hamadouche, "Automatic threshold selection in OS-CFAR radar detection using information theoretic criteria," *Progress In Electromagnetics Research B*, Vol. 30, 157–175, 2011.
7. Press, W. H., S. A. Teukolsky, W. T. Vetterling, and B. P. Flannery, *Numerical Recipes in C: The art of Scientific Computing*, 2nd edition, Chapter 8, Cambridge University Press, 1992.
8. Rohling, H., "Radar CFAR thresholding in clutter and multiple target situations," *IEEE Transactions on Aerospace and Electronic Systems*, Vol. 19, No. 4, 608–621, Jul. 1983.
9. Shor, M. and N. Levanon, "Performances of order statistics CFAR," *IEEE Transactions on Aerospace and Electronic Systems*, Vol. 27, No. 2, 214–224, Mar. 1991.
10. David, H. A. and H. N. Nagaraja, *Order Statistics*, 11–12, Wiley, New York, 2003.